Middle Ordovician acritarchs and problematic organic-walled microfossils from the Saq-Hanadir transitional beds in the QSIM-801 well, Saudi Arabia

Acritarches et microfossiles à paroi organique problématiques de l'Ordovicien moyen, à la transition Saq-Hanadir dans le sondage QSIM-801, Arabie Saoudite

Alain Le Hérissé[1], Claudia Guidat[1], Fabrice Not[2], Marco Vecoli[3], Pierre Breuer[3], Charles Wellman[4], Philippe Steemans[5]

[1]Université de Brest, UMR 6538 CNRS « Domaines océaniques », IUEM, CS 93837, Rue Dumont D'Urville, 29280 Plouzané, France alain.le.herisse@univ-brest.fr

[2]Plankton Group - UMR 7144 Station Biologique de Roscoff - CNRS & UPMC .Place Georges Teissier CS 90074,29688 Roscoff Cedex, France

[3]Biostratigraphy Group, Geological Technical Services, Saudi Aramco, Dhahran, 31311, Saudi Arabia

[4]Department of Animal and Plant Sciences, University of Sheffield, Alfred Denny Building, Western Bank, Sheffield S10 2TN, U.K.

[5]Laboratory of Palaeobiogeology, Palaeobotany, Palaeopalynology, Liège University, 4000 Liège, Belgium

Abstract

Core samples from the QSIM-801 water well, drilled in central Saudi Arabia, cover a 93-feet interval spanning the transition between the Sajir Member of the Saq Formation, that consists mainly of sandstones of tidal sand flat environment, and the Hanadir Member of the Qasim Formation, characterized by argillaceous graptolitic mudstones, corresponding to a tidal delta front. The samples contain abundant, exceptionally well-preserved and diverse palynomorphs which include cryptospores, acritarchs, chitinozoans, cuticle-like fragments, and other problematic organic-walled microfossils. The studied interval is biostratigraphically well constrained by the presence of chitinozoans of the *formosa* and *pissotensis* Zones of late early to late Darriwilian age (Middle Ordovician), in the uppermost Saq Formation and Hanadir Member. The biostratigraphic age of the Sajir Member considered to span the

Dapingian-Darriwilian boundary is re-discussed with results herein. The uppermost part of the Sajir Member yielded the ichnofossil *Phycodes fusiforme*. Acritarch assemblages from the Sajir Member of the Saq Formation are poorly diversified, dominated by sphaeromorphs. More diverse assemblages of acritarchs, associated with enigmatic forms, occur in the Hanadir Member of the Qasim Formation. The contact between the two formations, and the transition between the palynomorph assemblages, are sharp, suggesting a stratigraphic hiatus. The quantitative analysis allows to discuss the paleoenvironmental changes and possibly climatic changes and the hypothesis of ice house conditions during this period. Among the diagnostic acritarch taxa observed, are *Frankea Breviuscula, F. longiuscula*, *Baltisphaeridium ternatum*, *Dasydorus cirritus*, *Dicrodiacrodium ancoriforme, Poikilofusa ciliaris, Pterospermopsis colbathii* and *Uncinisphaera fusticula.* These are associated to other typical forms known to range across the Lower-Middle Ordovician boundary, such as *Aremoricanium rigaudae*, *Aureotesta clathrata*, *Barakella fortunata*, *B. rara, Baltisphaeridium klabavense, Glaucotesta latiramosa* and some *Striatotheca* spp. Galeate and peteinoids acritarchs are also well represented, as well as tiny forms of the ultraplanctonic size class. Three new species are proposed: *Frankea longiuscula* var*. darriwilense*, *Micrhystridium regulum*, and *Tyrannus proteus*. Repeated occurrences throughout the section of cryptospores, problematic microfossils such as organic filaments, cuticle-like tissues, striated and pigmented leiospheres frequently in clusters, are interpreted to reflect recurrent terrestrial and freshwater inputs in the depositional environment. Single-specimen, high-resolution analyses using Confocal Laser Scanning Microscopy on the enigmatic form *Tyrannus proteus* nov. sp. show fluorescence emission spectra and microstructural properties significantly different from those of typical marine acritarchs from the same levels.

Résumé

Les échantillons du sondage QSIM-801, foré dans la partie centrale d'Arabie Saoudite pour des recherches d'eau, couvrent un intervalle de 93 pieds, à la transition entre le Membre Sajir de la Formation Saq, avec essentiellement des grès, caractéristiques d'une zone intertidale sableuse, et le Membre Hanadir de la Formation Qasim, qui consiste en boues argileuses à graptolites de front de delta. Dans ces échantillons, les palynomorphes sont abondants et bien conservés, comprenant des cryptospores, des acritarches, des chitinozoaires, des fragments de

cuticules et d'autres microfossiles à paroi organique qui sont problématiques. L'intervalle étudié est bien contraint stratigraphiquement par la présence de chitinozoaires des zones à *formosa* et *pissotensis*, de la base à la partie supérieure du Darriwilien (Ordovicien moyen), dans le sommet de la Formation Saq et le membre Hanadir. L'âge du membre Sajir généralement considéré comme marquant la limite Dapingien/Darriwilien, est rediscuté avec les résultats de cette étude. Dans le sondage, la partie supérieure de la Formation Saq contient l'ichnofossile *Phycodes fusiforme*. Les assemblages d'acritarches du Membre Sajir de la Formation Saq sont peu diversifiés, dominés par des sphaeromorphes. Les acritarches sont plus diversifiés, associés à de nombreuses formes énigmatiques, dans le Membre Hanadir de la Formation Qasim. Le contact entre les deux formations et la transition entre les assemblages est abrupt, suggèrant l'existence d'un hiatus stratigraphique. L'analyse quantitative a permis de discuter les changements paleoenvironnementaux et de possibles changements climatiques, dont l'hypothèse d'un épisode glaciaire durant cette période. Parmi les acritarches les formes les plus intéressantes stratigraphiquement sont *Frankea breviuscula*, *F. longiuscula, Baltisphaeridium ternatum, Dasydorus cirritus, Dicrodiacrodium ancoriforme, Poikilofusa ciliaris, Pterosmermopsis colbathii* ou *Uncinisphaera fusticula*. Ils sont associés à d'autres formes typiques de la limite Ordovicien inférieur à moyen, comme *Aremoricanium rigaudae*, *Aureotesta clathrata, Barakella fortunata, B. rara, Baltisphaeridium klabavense*, *Glaucotesta latiramosa* et des *Striatotheca* spp. Les formes galeates et les *Peteinosphaeridium* sont également bien représentés, ainsi que de très petites formes de taille ultraplanctonique. Trois nouvelles espèces sont proposées, *Frankea longiuscula* var. *darriwiliense*, *Micrhystridium regulum*, et *Tyrannus proteus*. La présence répétée tout au long de la section de cryptospores, de microfossiles problématiques, comme des filaments organiques, des tissus ressemblant à des cuticules, des leiosphères striées et pigmentées, souvent en colonies, sont interprétés comme des apports récurrents du continent probablement par les rivières, dans l'environnement de dépôt. L'analyse en microscopie confocale de spécimens isolés de la forme énigmatique *Tyrannus proteus* nov. sp., montre des spectres d'émission de fluorescence et des propriétés microstructurales significativement différentes de celles des acritarches typiques présents dans les mêmes niveaux.

1. Introduction

Several keys papers published over the past years discussed the possibility of an “early Paleozoic Ice age” (Pohl et al., 2016), since the Darriwilian. This hypothesis could contradict the concept of long term global greenhouse climate stability in most of the Ordovician, before the cooling interval of the late Ordovician. Arguments of a glacial onset that may have occurred as early as the Darriwilian at the Gondwanan paleo South pole, predating the Hirnantian glacial maximum (Ghienne et al., 2007), are sedimentological, geochemical, micropaleontological or related to the paleogeographical configuration (Dabard et al., 2015; Thompson, 2011; Trotter et al. 2008; Turner et al., 2012; Pohl et al., 2014; Pohl et al., 2016; Rasmussen et al., 2016; Vandenbroucke et al., 2010 etc.).

The present contribution, deals with the Dapingian (?) To Darriwilian, from the transition between the Sajir Member of the Saq Formation and the Hanadir Member of the Qasim Formation, in well QSIM-801, in central Saudia Arabia, and it is interesting to consider, if whether or not the results we obtained after the palynological investigation, supported or failed to support this hypothesis of precocious cooling in the Middle ordovician

As previously discussed (Le Hérissé et al., 2007), the sediments of the borehole QSIM-801 yielded rich assemblages of marine palynomorphs (acritarchs, prasinophycean phycomata, chitinozoa), but also some cryptospores and microscopic plant remains. Many palynomorphs are also enigmatical, not previously described, and we discuss unreported minute microfossils of picoplanktonic and ultraplanktonic size classes, which are key components of the assemblages. The chitinozoa data provide a robust biostratigraphic framework, and we discuss also the biostratigraphic potential of the acritarchs and prasinophycean phycomata assemblages, in view to precise a still unsatisfactory biostratigraphic control for the Saq/ Hanadir transition in this area.

After the first occurrence of Middle Ordovician cryptospores were revealed in a stratigraphically equivalent interval in Saudi Arabia (Strother et al., 1996), more recent findings (Strother et al., 2015; Steemans et al., this volume) confirm their importance and the establishment of a vegetation phase and cover non negligible during this period. In QSIM-801 well, the percentages of cryptospores can reach values of 6 or more than 8 % of all the palynomorphs (see discussion).

The Hanadir shales contains also abundant amorphous organic matter (up to 30%), with subsidiary opaque material. These high burial rates of organic carbon during the Darriwilian, associated to the vegetation cover, could have had possible effects on the sedimentary processes and climate. The question is to know if they could have been sufficient to significantly drawn down atmospheric CO_2 and to cause transient cooling of the global climate.

To achieve a high temporal resolution and to discuss the specific characteristics of the assemblages, e.g. the abundance of minute palynomorphs, or over-representativity of some taxa, emphasis was also given on a detailed quantification of the variations in palynomorph assemblages, to reconstruct both terrestrial and aquatic changes along the succession, and the sea-level changes, in complement of the sedimentological data. The question is also to know the exploration potential of the Saq/ Hanadir transition and if the two formations can represent a good reservoir-seal (and source) assemblage as the Sarah Formation upwards and its overlying Silurian Hot shale.

2. Geological setting and biostratigraphy

Thick and well preserved Ordovician succession is exposed and penetrated on the eastern border of the Arabian Precambrian Shield (Fig. 1, Vaslet et al., 1987). In the regional lithostratigraphy, the Tabuk Formation of Steinecke et al. (1958), amended by Powers et al. (1966), is substituted now in ascending order by the upper part of the Saq Formation (also named Anz Formation by Khalifa, 1993, 2015), the Hanadir, Kahfah, Ra'an and Quwarah members of the Qasim Formation and glacial and periglacial deposits referred to as the "Sarah-Zarqa" Formation (Vaslet, 1990; Melvin, 2015). The Saq/Qasim are present or with equivalents into Jordan and southward in Oman (Stump, 1995; Al-Hajri, 1995).

The QSIM-801 well, drilled northwest of Riyad in the central part of Saudi Arabia (Fig. 1), penetrated a 1200 ft thick Ordovician sequence, to test the Saq aquifer and to evaluate the source rock potential of these series. The section studied is relatively short and concerns only a mid-Ordovician cored interval of 93 feet, penetrating from top to the bottom, the Hanadir Member of the Qasim Formation and the Sajir Member in the uppermost part of the Saq Formation.

We continue to use in this paper the global chronostratigraphy for the middle Ordovician proposed by Webby et al., (2004), and the succession Dapingian and Darriwilian, even though this scheme introduces many problems for intercontinental correlations. The difficulty is that the faunas used for the definition of stratotypes in deep-water facies of Canada and China are hardly recognized in inner-shelf facies of the south polar Gondwana and peri-gondawanan areas. For that reason, some regional scales have been recently reintroduced, e.g. the Bohemo-Iberian (= "Mediterranean") chronostratigraphical scale in the South Gondwana palaeobiogreographical region (Guttiérrez-Marco et al., 2016).

On the Arabian shield, the mid-Ordovician corresponds to increased subsidence that led to a major transgression with a maximum flooding surface, placed in the Darriwilian. The correspondence is upper part of the Arenigian, Oretanian to part of the Dobrotivian in the Bohemia-Iberian scale of Gutiérrez-Marco et al. (2016), The Darriwilian MFS, named O30, is comparable in importance to the S10 in the early Silurian (Haq and Al-Qhatani, 2005). Sharland et al. (2001) located MFS O30 within the Hanadir shale sequence and correlated it regionally across the Arabian Plate (Senalp and Al-Duaiji, 2001). According to the sedimentology, the limit between Saq and Qasim Formations in QSIM-801, was localized at 751 feet and corresponds to the transition between a tidal sand flat environment (Saq) and a distal delta front (Hanadir). In this core the Sajir sandstones-Hanadir shales contact is sharp and markedly erosional, compared to the contact throughout most of cored sections elsewhere in Saudi Arabia, where the transition is considered continuous and conformable. Going to the North of Saudi Arabia, a MFS is observed to the base of the Hanadir member. This one is not visible in QSIM-801.

Age assignments are of prime importance to calibrate the sedimentary and palynological events. The biostratigraphic age of the Sajir Member is considered to span the Dapingian-Darriwilian boundary, but with the palynological results of this study, and particulalrly the distribution of chitinozoa, this age is reconsidered. Ichnofossils of interest regionally in Saudi Arabia, such as the *Cruziana* or *Phycodes fusiforme*, occur in the upper part of the Saq formation, particularly in sandstones of core 8 of QSIM-801. The Hanadir shales contain some graptolites, *Didymograptus* cf. *bifidus* and *Didymograptus protobifidus* (Helal, 1964; Powers, 1968), some ostracods, conodonts and trilobites (Vaslet et al., 1987) and some trace fossils to the

Saq/Hanadir boundary (Khayal and Romano, 1988; Seilacher, 2000). The details of sedimentary facies and faunas have been described in a previous paper (Le Hérissé et al., 2007), and supplementary informations on other localities are also found in Ghavidel-Syooki et al. (2014) and Gutiérrez-Marco et al. (2016), in a comparison between neighbouring areas. The age of the Hanadir member, originally regarded as early Ordovician (Helal, 1964), was re-assigned on palynological evidence to the Darriwilian, i.e. upper Arenig to Llanvirn in the British terminology (Al-Hajri, 1995). In QSIM-801, and other boreholes, the chitinozoa of the *bulla* event, of early Darriwilian age, recognised as a deepening pulse on the Northern Gondwana domain, will be represented in the uppermost part of the Saq Formation (Paris unpublished data, Paris et al., 2007). This will be a first contradiction with a Dapingian age attributed to the upper Saq Formation in the regional charts. It is clear that the situation in the interval Dapingian to early Darriwilian is complex all over the world (Guttiérez-Marco et al., 2013, 2016), but with more accuracy on the Arabian margin of Gondwana, with condensed sequences and stratigraphical gaps, e.g. in Oman (Molyneux et al., 2006), in Iran (Ghavidel-Syooki et al., 2014), and Saudi Arabia.

In QSIM-801, our chronostratigraphical control is mainly established on the superposition of chitinozoan biozones. The first appearance and good representativity of *Siphonochitina formosa*, in the uppermost Saq Formation, at 759.6 feet, top of core 8 and higher, give the oldest assemblage. In the north Gondwana, the species *Siphonochitina formosa* is considered the index species of the eponym zone, dated late early Darriwilian, equivalent to *D.artus* graptolite Zone, and associated to a major flooding episode (Paris et al. 2007). The zone and the flooding are also known in Oman (Molyneux et al., 2002) and south eastern Iran, but in the last area it occurs after an important hiatus of the Dapingian and early Darriwilian (Ghavidel-Syooki et al., 2014).

It is possible to have a precocious appearance of *Siphonochitina formosa* in Saudi Arabia in the late Dapingian to earliest Darriwilian, but this need to be confirm by future analysis. The other possibility is that this part of the uppermost Saq in QSIM-801 is already late early Darriwilian in age, corresponding to the *formosa* flooding event of the chitinozoan-based calibration of early-mid Ordovician transgressive events of northern Gondwana (Paris et al., 2007). This situation in the upper part of the Saq Formation, was previously reported from other localities in Saudi Arabia, as

mentioned by Guttiérrez-Marco et al. (2013, p.4), where an unusal assemblage of chitinozoans from the *?D.ornensis* to *B. henryi* biozones and conglomeratic beds with lingulids are overlain by bedded sandstones yielding the first middle Darriwilian graptolites (El-Khayal and Romano, 1988; Al-Hajri, 1995). The upper part of the studied section in QSIM-801, from cores 3 to 1 (699.9-675.1 feet) is more evidently dated late Darriwilian, referred to the *pissotensis* chitinozoan biozone, which coincides also *pro parte* with a transgressive event.

With the duration of less than 3 Ma for a chitinozoan biozone (Paris et al., 2007), and probably the *pissotensis* biozone is not complete in the sequence of QSIM-801, we realize that the late Dapingian (?)-early Darriwilian to mid to late Darriwilian sequence in the QSIM-801 section is very condensed, in less than 100 feet. The situation suggests very high frequency sequences, and is also complicated by the existence of several discontinuities, as it has been confirmed by the sedimentary analysis (… ref. name sedimentologist or the study need to stay confidential?).

3. Material and methods

A total of 42 samples have been collected across the boundary between the Saq and Qasim Formations in QSIM-801 well, with a variable vertical resolution. All the samples were processed using standard palynological techniques. A first serie of samples was treated in the palynological laboratory of Aramco, and first results on this material have been published by Le Hérissé et al. (2007). Another serie of samples has been treated for this study, in the palynological laboratories of Brest and Liege, following globally standard palynological techniques, but also very soft acid digestion to try to obtain more complete specimens (e.g. with possible connections between specimens) of the most enigmatical forms. In Brest, research of tiny forms of palynomorphs were also engaged on no filtered residues.

In addition to conventional transmitted light microscopy, scanning electronic microscopy and confocal laser scanning microscopy (CLSM) have been applied to the material on a selection of species, for details of morphological features. Each species examined was characterized by two fluorescent spectral profiles, with a specific colored bullet. They both illustrate variations of excitation of the autofluorescence on several parts of the specimens.

The CLSM microscopy was mainly used to discuss the variations in autofluorescence spectra between the enigmatical form *Tyrannus proteus* nov. sp., and other species assigned to acritarchs. Confocal laser scanning microscopy (CLSM) is an important technique largely used in the biomedical sciences to image in situ cellular material to micro and nano-scale resolution (Pawley, 2006). In geological sciences the CLSM has most often been used for imaging delicate morphological features of palynomorphs (e.g. Feist-Burkhardt, S., and Pross, J., 1999). The CLSM in Brest was a Zeiss LSM 780, x50 Epiplan Apochromat objective AN 0.95, using Ar 405 nm excitation.

Quantitative changes in palynomorph assemblage composition and diversity were also measured within the cored section, with a count of at least 300 palynomorph specimens per sample. The relative abundance of each of the 46 taxa and groups recognized are shown for each sample in Tables 2 and 3. Relative abundance of amorphic organic matter (AOM) compared to palynomorphs has also been established separately. Amorphous organic matter comprise all particulate organic components that appears structureless at the scale of light microscopy.

Pyrite framboids and sulfur-rich nannospheres can be abundant in the organic residues, particularly in the Hanadir Member. This sedimentary pyrite can be formed by the reaction of H2S produced by bacterial sulfate reduction with detrital iron minerals, and decomposition of organic matter, and can indicate a chemically reducing deposition environment under anoxic conditions (Raiswel and Berner, 1986), in the Hanadir Member. Abundant and well-preserved AOM (concentrations in Table. 2), are frequently coupled with pyrite. It confirm Hanadir member is mainly preserved in anoxic conditions. But the fluctuations in percentages of amorphic matter and marine or terrestrial palynomorphs in QSIM-801, also suggest periodic expositions to dysoxic conditions. The organic matter of Hanadir member is highly mature type II kerogen with range of total organic carbon (TOC) between 0.5 to 2.98% (Ghazwani, 2012), that indicates the source rock of the Hanadir is in gas generation windows.

All illustrated specimens (Plates 1 to 7), from palynological slides prefixed SA 8219 (Turabah-1 Well), SA 44845, 44850, 44851, 44852.2, 44853.2, 44857.2, 44858.2, 44861.2, 44862.2, 44881, 44881.2, 44883.1, 44883.2, 44888, 44888.2, 44890,

44891.2, 44894.2, and LPB 13071 to 13085, are deposited in the collections of Saudi Arabian company in Dharhan, and the Laboratoire de Paléontologie de Brest (LPB), France.

1. Systematic paleontology

Two new species and one new variety of acritarchs are described and one species is revised. All palynomorphs taxa mentioned in the text are listed with authorship in alphabetical order in Appendix A

Algae Incertae sedis

Group ACRITARCHA Evitt, 1963

Genus ***Focusphaera*** Quadros, 1986

Type species: *Focusphaera elongata* Quadros, 1986

Focusphaera elongata Quadros, 1986, Plate 1, Figs. 12, 15

2007. ?*Tinacula* sp. A, Le Hérissé, Al-Ruwaili, Miller, Vecoli

Description : vesicle piriform, elongate in outline, base subspherical and unobstructed neck-like extension. The surface of the vesicle varies from microgranulate, reticulate, baculate or with pilosity The open distal end of the neck-like structure is simple or slightly constricted.

Remark: The first specimens mentioned in Le Hérissé et al., (2007) were mis-identified in ?*Tinacula* sp., before discussions with L. P. Quadros and evidence of analogy of this material with *Focusphaera elongata*. By this way, the middle Ordovician from Saudi Arabia shows interesting elements of comparison with the middle Ordovician of the Benjamin Constant Formation in the Solimões Basin, Brazil (Quadros, 1986a, 1986b, 1988; Le Hérissé, 2015, unpublished). The Hanadir Member of the Qasim Formation in Saudi Arabia, of Darriwilian age contains also *Barakella fortunata* and *Striatotheca rarrirugulata*, both likewise found in the Solimões Basin. Other specimens of *F. elongata,* than those illustrated there, are illustrated in Le Hérissé et al., 2007 (Plate 2, fig. 10-12).

Dimensions: (c.a. 55 specimens) total length from 36 to 75 µm, subspherical vesicle 29 to 45 µm in diameter, distal end opening 12 µm when constricted to 18 µm.

Occurrence: restricted to the Hanadir member, from top of Core 7 to core 1, Zone 3, mid to late Darriwilian.

Genus ***Frankea*** (Burmann, 1970) Servais, 1993 emend

1970 *Frankea* Burmann p. 292

1993 *Frankea* Burmann emend, Servais, p. 80

1995 *Fatkia* Vavrdová, p. 368

Type species: *Frankea hamata* Burmann, 1970 by original designation

Original diagnosis: Der Zentralkörper ist triangular, mit dreistrhliger Anordnung von Fortsätzen, die terminal an eimen gemeinsamen Ansatzpunkt in unverzweige Anhänge aufgabeln. Die Anzahl der terminalen Fortsatznhänge (Zwei und mehr) und das Längenverhältnis von Fortsatz zu Zentralkörper sind variabel (Burmann, 1970).

Translation of the original diagnosis: The central body is triangular, with a triradial arrangement of the processes which split distally from simple point into unbranched pinnae. The number of the terminal pinnae (two or more) and the ratio of process length to central body diameter are variable.

Emended diagnosis: Vesicle sub-circular to triangular in outline, bearing generally three processes, but sometimes only two or four. The processes are cylindrical, hollow, of various size, but relatively constant length for each specimen. The processes are in free communication with the vesicle interior, but the communication can be restricted for the species showing a plug to the base of the processes. One process can be simple The processes split distally from a single point into two to more pinnae. Sometimes one process can be simple. The surface of the vesicle and of the processes is smooth to granulate or striatogranulate. Opening by means of an epityche.

Remarks: Servais (1993, p.81) underlined the importance of the number of terminal pinnae and the ratio of process length to central body diameter for circumscription

and differentiation of the species of *Frankea*. Other observations (Vecoli et al., 1999) and the material studied here, do not support this assertion.

The vesicle wall thickness is varying. For the specimens thin-walled, i.e. the majority of the species described, the communication between the processes and vesicle interior is evident. But some specimens show a strong contrast between a thicker-walled vesicle and thickening extension at the base of the processes and a thinner wall for the rest of the trunk of the processes up to the top. This suggest, for some species, a sharp separation between process and vesicle cavities.

The genus was proposed by Burmann (1970), using thin sections, and of particular interest is one of the figuration proposed for *Frankea longiuscula*, Plate 2, fig 12, that clearly shows a thicker-walled vesicle. The successive emendations of the genus by Colbath (1986) or Servais (1993, or the discussions and remarks on the genus by Fatka et al. (1997) or Vecoli et al. (1997), do not provide any information about the importance of this feature, that is specially recognized in some specimens of *Frankea longiuscula*. We consider this question with the description of *Frankea longiuscula* var. *darriwilense* var. nov.

Frankea longiuscula var. *darriwilense* var. nov., Plate 3, Figs 1-4, 7, 9, 11, 12; Plate 6, Fig. 6

1970. *Frankea longiuscula* Burmann, Plate 2, fig. 12, Plate 3, 1, 2.

1977. *Multiplicisphaeridium longiusculum* (Burmann) Eisenack, Cramer and Diez in Cramer and Diez, Plate 6, Fig. 16.

?1999. *Frankea longiuscula* Burmann, 1970, Vecoli, Tongiorgi, Playford, Plate 2, 2.

?2000. *Veryhachium subglobosum* Jardiné et al., 1974, Molyneux and Al-Hajri, Plate 2, b.

2007. *Frankea longiuscula* Burmann, 1970, Le Hérissé, Al-Ruwailii, M., Miller, M. and Vecoli, M., Plate 1, Figs 12, 14, 15.

Derivation of name: From Darriwilian, stage of the Middle Ordovician.

Typification: Holotype, QSIM-801 well, level 715.6 feet, core 4, slide SA 44861.2 (EFS48/1), Plate 3, Fig. 7

Type locality and horizon: QSIM-801 borehole, Hanadir Shale Member, Quasim Formation, Middle to late Darriwilian.

Diagnosis: A variety of *Frankea Longiuscula* Burmann, 1970, which differs in having a darker and thicker-walled vesicle, and an important variability in the termini of processes, in the form and number of pinnae.

Description: Vesicle subtriangular to subcircular in outline, with convex sides, bearing three long and cylindrical processes (rarely one additional process present), one located at each angle of the vesicle. The processes are distally simple or splitting into two up to 12 pinnae. The vesicle and proximal part of the processes are distinctly darker and thicker than the rest of the processes. Vesicle and process surface smooth to microgranulate. Excystment by means of an epityche (horse-shoe opening) between two processes.

Dimensions: (c.a more than 500 specimens), Vesicle diameter 29 to 61 µm, process length 45 to 92 µm, width 2,5-3 µm, pinnae between 5.5 and 11 µm; Vesicle wall thickness 1.2 µm.

Remarks: The first remark concern the good representativity of this variety in the material of zone 2 and 3 (late early to late Darriwilian), attaining 10% up to 15% of the total assemblage in several levels, without equivalent for another species, only for groups (Leiosphaerids, galeates, *Micrhystridium* spp, *Veryhachium* triapsidate. etc.). The high percentages are intermittent in the succession, suggesting recurrences of “blooms”.

This taxon is characterized by well developed processes, but also some important morphological variations and a proportion of aberrant specimens

Apart from the illustrations of Burmann (1970) that suggest more important variability in *Frankea longiuscula* than indicated in the original description, Cramer and Diez (1977, p.350) noted in the material of Morroco some *Frankea longiuscula* consistently darker and thicker-walled, that they consider to be possibly a separate species. Because we have in our material some true *Frankea longiuscula*, thin-walled, without darker vesicle wall, we suggest darker and thicker-walled forms not as new species but as indetermediate forms clearly different with the type. By separating them at variety level, as a subspecific category according the definition of Servais and

Molyneux (1997), we provide also information useful locally for the stratigraphy and the paleoenvironmental interpretation, taking account of the limited distribution of this variety and its quantitative importance.

If darker vesicle wall and darkened base of the processes is consider significative to the specific rank, e.g. for *Veryhachium checkleyensis* Dorning, 1981, in the Silurian, it is also the character of intermediate forms inside the genus *Lusatia* and the species *Lusatia dendroidea* from the late Cambrian: “The free communication of processes with the vesicle interior is evident in translucent and thin-walled specimens. Specimens with a dark, thick-walled vesicle and thin-walled processes may simulate a separation and give impression of a biilayered vesicle. The darker area may extend shortly into the base of the processes….” (Albani et al., 2007). It is evident that with its variable morphology, with only one process, two processes (bipolar forms) or three processes, and its variable vesicle thickness and variable branching, *Lusatia dendroidea* show some analogies with *Frankea longiuscula* var. *darriwilense*. *Lusatia heteromorpha* of Vavrdová, 1986, described in the Early Llanvirn of the Prague Basin, differs by capitate terminations of pinnae and a granular central body.

Another possible comparison, considering the variability, is with the lower to middle Ordovician genus *Dicrodiacrodium*, for which the contact between process base and central body is with or without plug (Servais et al., 1996). All specimens observed in QSIM-801, in the mid to late Darriwilian, have a plug to the base of processes, the specimens differing only by the varying length of the polar process. But in the discussion of variability inside *Dicrodiacrodium* by Servais et al.(1996), no indication is provided on the temporal distribution of specimens showing a basal plug on the processes, to judge about its biostratigraphical importance.

In complement of an intensive polymorphism, some aberrant forms of *F. longiuscula* var *darriwilense* have been observed (e.g. Pl. 3, Fig. 9), all along the section. In QSIM-801, the malformations affected preferentially *F. longiuscula* var. *darriwilense* in QSIM-801 material, which is also overrepresented. But other malformed specimens have been encountered, e.g. for some species of the genus *Veryhachium.*

Previous records: The material of Burmann is recorded in the supposedly upper Llanvirn from eastern Germay. In Cis-Sahara Morroco, *Frankea*

(*Multiplicisphaeridium) longiusculum* was recorded in the Tadla Basin, in the Late Arenigian by Cramer and Diez (1977) in a material redated late Dapingian to Darriwilian by chitinozoa (Soufiane and Achab, 1993). We supposed some *F. longiuscula* mentioned in the literature are possible *F. longiuscula* var. *darriwilense*, e.g some specimens published by Vecoli et al., 1999, taking account of the break seen in basal part of some processes, suggesting the existence of a basal thickening. But this need some revisions. The material of Vecoli et al. is from the *Didymograptus murchinsoni* graptolite Zone, that supports an early to mid-Darriwilian age (Zalasiewicz et al., 2009), quite consistent with the distribution of *F. longiuscula darriwilense* in QSIM-801.

Occurrence: Uppermost part of the Saq Formation and Hanadir Member of the Qasim Formation in QSIM-801 borehole, Late early to late Darriwilian.

Genus ***Micrhystridium*** Deflandre, 1937

Type species: *Micrhystridium inconspicuum* (Deflandre, 1937) Deflandre 1937 by original designation

Remark: we concur with other authors that Sarjeant and Santcliffe's 1994 (p. 22-23) emendation of *Michystridium* is too broad to be used, with unacceptable characteristics, such as wall uni or bilayered. Accordingly, *Michystridium* concern small forms of acritarchs, spherical to subspherical with wall single layered and simple hollow acuminate processes with free communication into vesicle interior.

Micrhystridium regulum sp. nov., Plate 7, Figs. 2-6

Derivation of name: latin *regulum*, petty king, referring to the little size of this species.

Typification: Holotype, QSIM-801 well, core 1, level 749.9 ft., slide SA 44891.2 (E61).

Type locality and horizon: QSIM-801 borehole, central Saudi Arabia, Uppermost Saq Formation and Hanadir Member of the Qasim Formation, late early to late Darriwilian.

Diagnosis: Vesicle originally spherical, outline circular to subcircular, distinct from processes. Wall single layered, 0,5 µm thick, psilate. Between 7 to 12 homormorphic processes, cylindrical, quite large, clearly differentiated from the vesicle cavity and with contact angular, wall psilate, tapering to acuminate tips. Excystment structure not observed.

Remarks and comparison: *Micrhystridium regulum* sp. nov. present processes variable in size and number, and two morphotypes are distinguished: one with short processes, mainly in the Saq Formation, the second with longer processes in the Hanadir Formation. Among the different species of *Micrhystridium* recorded in this material, many have simple morphology, and are difficult to assign to established species, the observed variation involving only size, length and number of simple processes, without ornamentation on the vesicles. The species *M. regulum* is different and unique, and in spite of a small size is easy to distinguish in optical view and SEM, from the others *Micrhystridium*.

Dimensions: (c.a.10 specimens) Diameter of vesicle 3 to 6,5 µm, length of processes 1,5 to 5,5 µm

Occurrence: Uppermost part of the Saq Formation, and Hanadir Shales Member of the QSIM-801 well, Acritarch Zones 2 and 3, Late early to Late Darriwilian.

Genus ***Tyrannus*** Wood and Tekbali, 1987

Type species: *Tyrannus giganteus* (Jardiné et al., 1974) Wood and Tekbali, 1987

Tyrannus proteus sp. nov., Plate 5, Figs. 1-13

2007. *Tyrannus* sp. A, Le Hérissé, Al-Ruwaili, Miller, Vecoli

Derivation of name : latin proteus, proteiform, for the variable aspect of the specimens referred to this species

Typification: Holotype, QSIM-801 well, level 693.1 feet, core 2, slide SA 44853.2, (EF U47/2), Plate 5, Fig. 11

Type locality and Horizon: QSIM-801 well, Central Saudi Arabia, Hanadir Shales Member of the Qasim Formation, Miiddle to Late Darriwilian.

Diagnosis: Vesicle hollow, wall thick, unilayered, surface psilate, subtriangular to subcircular or subpolygonal in outline, depending on the numbers of processes. Two to eight processes, cylindrical to conical, hollow, communicating freely with the central cavity, distally truncate and open. The distal extremities of the processes appear to be thinner and ligther in color.

Dimensions: (c.a. more than 100 specimens), vesicle 75 to 125 µm in diameter, process length 25 to 50 µm, process width 10 to 15 µm, overall diameter 90 to 200 µm.

Remarks: With previously described specimens (Le Hérissé et al., 2007) a large number of *T. proteus* sp. nov has been observed and studied in the new material from QSIM-801, in optical view, SEM and CLSM. A similar material has also been seen in the Middle Ordovician of core Turabah-1. The new specimens of QSIM-801 were recovered using a gentle preparation procedure, better than conventional palynological processing. Objective was to try to establish if some specimens could be found in connection, by open-ended processes. But all specimens represented in the majority of samples studied, were solely found isolated. These findings seem to confirm that *Tyrannus proteus* sp. nov. possesses all the features of unicellular organism, as vegetative stage, cyst stage or spore.

The generic attribution to *Tyrannus* is based on several important characteristics: the large size of these specimens, the light brown coloration of the wall of *T. proteus*, as for the type species *T. giganteus*, in contrast to the others palynomorphs and particularly acritarchs in the same preparations, and processes distally opened. Pronounced instraspecific variation and polymorphism is another characteristic of *T. proteus*, which distinguish the species from the majority of the acritarchs, with exception of *Frankea longiuscula* var. *darriwillense* (cf. discussion for this variety). This phenotypic plasticity is on the form and number of processes, not on the size, because the size distribution does not reveal any distinctive size groups. This kind of variation could likely be discussed environmentally induced, may be under conditions of changing salinity, as we suggested for the succession.

The study of isolated specimens of *T. proteus* by CLSM (cf. Plate 6, Fig. 7, 8) , compared to results on acritarchs in the same level was interesting. Each species examined, two *Stelliferidium* spp., a *Frankea longiuscula* var. *darriwilense* and *Tyrannus proteus*, was characterised by two fluorescent spectral profiles with a specific colored bullet. These profiles both illustrate variations of excitation on different parts of the specimens. It can be noticed some differences in fluorescence intensity: between the profiles of the *Stelliferidium* and *Frankea*, quite similar, and the profiles of *Tyrannus proteus*. Because they do not seem to be related to thermal alteration, they suggest a difference in origin or preference in environment between the acritarchs and *Tyrannus proteus* that could be of influence in the fluorescence signal.

The distally open processes and polymorphism could suggest comparisons between *Tyrannus proteus* and the *Tappania/Germinosphaera* organisms, possible fungi, described in the Neoproterozoic (Butterfield et al., 1994; Butterfield, 2009). But our gentle processing of samples does not confirm evidence of hyphal fusion as for the *Tappania* and *Germinosphaera*, and the analogies are only convergence of form.

Occurrence: The first specimens are recorded in the uppermost part of the Saq Formation, but the species is more common in the Hanadir Shales Member of the QSIM-801 well, Acritarch Zones 2 and 3, late early to Late Darriwilian.

Distribution: Uppermost part of the Saq Formation, and Hanadir Shales Member of the QSIM-801 well, Acritarch Zones 2 and 3, late early to Late Darriwilian.

2. Composition of palynomorph assemblages

The samples contain a rich palynoflora of marine palynomorphs, acritarchs and prasinophycean phycomata and also chitinozoa, mixed with possible freshwater algae, but also terrestrial elements, e.g. cryptospores, which are described in a separate paper (Steemans et al., this issue). Some forms encountered have never been described, making it difficult to infer their depositional environment, marine or non-marine. In the samples we have identified for example some grey to dark microfossils, not referred to phytoclasts. They are described and illustrated as unidentified dark-grey bodies. We have also the evidence in this material of very

small microfossils of the picoplanktonic and ultraplanktonic size classes, very abundant, and we discuss their depositional distribution and paleobiologcial significance.

Acritarchs and prasinophytes assemblages are rich, well preserved all along the section, even though in some samples the palynomorphs can be strongly affected by pyritisation. A total of 72 species have been identified, attributed to 37 genera (Table. 1). They serve to propose a biozonation of the Saq/Hanadir transitional beds, and the associations are compared to associations described elsewhere. Finally, variations in both marine and terrestrial elements, are analysed from counts of species, genera, groups of palynomorphs, but also relative abundance of amorphous organic matter, to appreciate the paleoenvironmental changes along the section (Tables 2 and 3).

2.1. Unidentified dark-grey bodies

Small, relatively uncompressed remains, dark-grey in color are found in many samples studied. The dark grey color is characteristic and is considered to be diagnostic of these elements, but they do not have characteristics of charcoal fragments such as splintery facture, silky lustre or specific internal anatomy (Scott, 1989, 2010).

Two different morphological types have been recognised.

Type 1 (Plate 4, fig. 1),

Description: complex palynomorph with a bipolar symmetry, composed of a central body, sub-spherical, hollow, highly colored, extended to the poles by a thin cylindrical outer membrane. This membrane is attached to the central body. No opening observed.

Dimensions: central body 50-60 µm in diameter; membranous expansions to the poles, 25 to 78 µm in length.

Type 2 (Plate 4, figs. 2-5),

Description: when complete the palynomorph is also bipolar, subspherical, outline circular to oval in polar view, composed of two halves, with a structure rounded and

membranous expansion in the central area of the polar zone. The ornamentation consists of radial striae in the polar zone and of concentric granular ridges towards the equatorial zone.

Dimensions: Complete specimens 45x90 µm to 70x100 µm in total length and width; isolated halves 69 to 80 µm in diameter

Remark: Many specimens of Type 2 have been recorded only as detached halves.

Discussion and comparison: The specimens described above as Type 1 resembles to the Silurian acritarch *Carminella maplewoodensis* Cramer, 1964, by the general construction, a central body surrounded by a cylindrical membrane. But they differ by: a more large size; a central body not covered by filose processes; and the cylindrical membrane not open-ended. The specimens of Type 2, also resembles to the early Devonian acritarch *Riculasphaera fissa* Loeblich and Tappan, 1969, with the mode of opening by equatorial splitting, but polar ornamentation and sculpture are different. The most reliable taxonomic feature of this material is its light grey to dark grey color when accompanying acritarchs, prasinophycean algae and cryptospores, are continuously pale and light yellow in color, indicating no evidence of thermal alteration in this material. The opacification of the light grey to dark grey material could also be derived from prolonged transport of a continental or freshwater material in the marine environment, under possible oxydating conditions. But, as previously mentioned, post-depositional alteration do not affect the other palynomorphs. Another hypothesis will be to associate these palynomorphs to sediment reworking, which exist for acritarchs in some levels. But there is no evidence of acritarchs reworked in the 37 levels, on a total of 42, where the light grey to dark grey elements are represented.

Some similarity exist between these light grey to dark grey elements and some modern freshwater algal spores such as *Gelasinicysta* among the Zygnemataceae, that are spheroidal to discoidal and composed of two equal halves separated by an equatorial suture (Head, 1992), as for Type 2 recognised herein.

5.2. Distribution and importance of minute palynomorphs

The importance of small phytoplanktonic forms is well established in oceans today and they play crucial roles as primary producers, bacterial grazers and parasites

(Barber and Hilting, 2002; Not, 2004). The scheme for classification of marine microorganisms according to size was delineated largely based on sieving technology. Sieburth et al. (1978) split microorganisms into three categories and

gave a definition of microplancton (more than 20 µm) and nannoplankton (2 to 20 µm) and added the term picoplankton for organisms less than 2 µm. The term ultraplankton, also used herein, was added later by Murphy and Haugen (1985), defined as the sum of picoplankton and nannoplankton (between 0.2 to 15-20 µm), which represents the size range of the minute palynomorphs also observed in the QSIM-801 material. The term ultraplankton is globally equivalent to the term ultramicroplankton of Tappan (1980).

Acritarchs and sphaeromorphic palynomorphs, smaller than 10-15 µm in overall diameter, are detected in many residues of the Paleozoic, but neglected because their small size or moderate interest for biostratigraphy. They effectively can be loose when workers are using sieving. But, in the geological record we can question the real abundance and importance of these elements, and their availability to be preserved, during and after deposition, by comparison to living picoplanctonic and ultraplanctonic forms and classes, in modern oceans and sea water masses. Servais et al. (2016) said: “the fossil record of the phytoplankton is biased by a huge mesh-size effect and reports of fossil phytoplankton <20 µm – picoplankton and in particular of bacterioplankton – are virtually absent”. Servais (2016), also asked for a picopaleontology. The problem is that these authors stay to the level of the concept, and do not demonstrate the true part of bacterioplankton, picoplankton and ultraplankton in fossil residues. The fossil record of the minute palynomorphs, in the Proterozoic and Paleozoic, is in reality very rare and limited at this moment, as discussed below.

After the record evidence of possible cyanobacteria, of abundant small acritarchs and sphaeromorphic palynomorphs in the material of Dapingian(?) to late Darriwilian in QSIM-801, we have first establish the distribution of the size classes of the different elements preserved. The purpose was to identify their diversity, to classify them and to apply the good terminology to describe them. Finally we discuss their significance. Some elements are illustrated on Plate. 7.

Body-size trends of the acritarch and sphaeromorphic palynomorphs in QSIM-801 material

A simple approach has been used for the measurements of the microfossils, taking account of the total diameter, i. e. sum of central body diameter+length of ornaments to the surface. We provide an example (Figs. 2, 3) of counts for two samples of QSIM- 801 well: a total of 2250 microfossils counted for the level QSIM-801, 758 ft., core 7; a total of 920 microfossils counted for QSIM-801, 712.7 ft, core 4. The counting was on 5 slides of each sample.

The figures 2 and 3 demonstrates that a very large distribution of body sizes coexist in the samples, but permit also a clear partitioning of size variations in the sequence. Two interesting classes of size can be isolated: the first one with ultraplanktonic forms less than 10 µm, representing 6 to 16 % of all the palynomorphs; the second concern ultraplanktonic and microplanktonic forms of 10 to 20 µm in size, which represents 14 and 15% of all the microfossils. And many forms, 70 to 79 % of all the palynomorphs (with chitinozoans, siculae of graptolites etc. for the more large elements), have a mean size of more than 20 µm.

Two important peaks of abundance are also indicated for the small forms, between 4 and 6 µm and between 18 and 22 µm, separated by a zone where microfossils are less abundant, with mean size values of 12.5 to 14 µm.

The overall trends do not differ greatly between the two samples of Figs. 2 and 3.

In complement, the use of microporous filters less than 5 µm, apparently show quasi absence of small acritarchs and leiosphaerids between 1 and 4 µm, but have allowed to detect a class of nannospheres, of few hundred of nanometers in diameter (less than 1µm).

Minute palynomorphs categories

Three main categories of minute palynomorphs have been distinguished: the nannospheres, with a mean size less than 1 µm; the acritarchs and small sphaeromorphs, with a total diameter between 5 and 20 µm; the clusters of minute palynomorphs that are either interpreted as terrestrial spore masses, possible spores

of chlorococcales, clusters of small prasinophycean algae or other microalage, which are aggregates of small units of 6 to 15-20 µm in diameter.

The combination of SEM and conventional light microscopy were found to be the most adequate tools for the analysis of minute palynomorphs, even thought many of the smallest forms, for example the bacteria, remain very difficult, or even impossible, to differentiate by light microscopy. They are only seen when they are attached to decaying organic matter mats (Pl. 7, fig. 14). CLSM has also been used, but this tool appear insufficiently precise and clearly less informative than SEM at high magnifications. The difficulty for the study of fossil material by CLSM in Paleontology, compared to Biology, is that we do not have possibility of amplification of the fluorescence signal by use of markers.

Nannospheres

The nannospheres were in nature the smallest elements identified in the material of QSIM-801 well, with a size between 0.2 to 1 µm. They have been extracted from water residues passed through 3 to 0.8 µm Nucleopore Polycarbonate filters (Plate 7, Figs. 15, 16). They are clearly differentiated from the pyritic spheres with framboidal structures, such as *Bavlinella foveolata* (or *Sphaerocongregus variabilis*) which are also found in these levels rich in pyrite, but not illustrated herein. In optical view nannospheres appear stained, possibly rich in sulfures, like the accumulations seen in modern freshwater deposits and illustrated by Lepot et al. (2014). They seems to be equivalent to the smallest (< 1 µm) nano-scale spheroids described from the Neoproterozoic black shales of the Ediacaran Doushantuo Formation in China (Borjigin et al, 2014). It is suggested they are comparable to cell envelopes of cyanobacteria.

Small acritarchs and sphaeromorphs

Small acritarchs, and small sphaeromorphs isolated in the matrix, are also present throughout the section in significant proportions, and they represent the second category of minute palynomorphs observed in the material.

Plate 7, figs. 5, 6, 7, 8, 9-10, 12, shows some examples of the smallest forms of acritarchs and leiosphaerids, seen in the material. These ones have a total diameter between 5 to 9-10 µm. They are equivalent in size, for the Paleozoic, to the

specimens illustrated by Munnecke and Servais (1996), from polished rock samples of the Silurian of Gotland, that have size between 5.5 and 10 µm (1996, Plate 4, figs. 1, 2, 4). But the elements described by these authors, do not have size of picoplankton as mentioned, because they are too large, more than 2 µm, according the definition of size range for the picoplankton. They need to be described as ultraplanctonic forms. They are equivalent to forms seen in the same material (without sieving) by Le Hérissé (1989), but not described by “parti pris”, of time and objectives. One example of a small acanthomorph of 5 µm is seen, for example, hooked on a *Eupoikilofusa rochesterensis* (Le Hérissé, 1989, Pl. 13, fig. 7).

Agic (2015), provided another example of minute palynomorph in the Palaeozoic, the early Cambrian of Estonia, with the description of a new species of small acritarch with a porous wall structure, *Reticella corrugata*. The size is between 4 to 10 µm. It is suggested by the author that *Riticella* will testify the presence of eukaryotic picoplankton or picoprasinophytes as early as the Early Paleozoic, but as previously commented, the right terminology for these tiny fossils is ultraplanktonic forms not picoplanktonic.

Many acritarchs from the Upper Vendian-Lower Cambrian of the East European Platform in Poland, described by Moczydlowska (1991) are also of small size but mainly in size range of more than 10 µm and up to 20-30 µm, a size that attains size of microphytoplankton. The smallest form described in this work is *Helosphaeridium radzynianum*, with an overall diameter of 9 to 12 µm.

It is interesting to consider, for the material of QSIM and the references above that two fractions of size are distinguished for the small acritarchs: one up to 10 µm, the second between 10 and 20-30 µm. The smallest forms, by opposition to the microphytoplankton have a high surface/volume ratio, which is considered a selective advantage, e.g. under oligotrophic or reduced light conditions (Prauss, 2000).

We can compare with the Mesozoic and Cenozoic, where several references to small acritarchs and prasinophytes are found, in the Middle and late Triassic (Roche, 1994; Brocke and Riegel, 1996; Feist-Burkhardt et al., 2007; Götz and Feist-Burkhardt, 2012; Riegel et al., 2014), the Jurassic (Courtinat, 1983), the Cretaceous (Habib and Knapp, 1982; Schrank, 2003), or the Neogene (see reference in Head, 2003). These studies show the same fractions of size than in the QSIM material and other

references in the Paleozoic, with two distinctive sub-groups, one concerning the ultraplankton and the other with sizes between ultraplanktonic and micropalnktonic forms. The difficulty, when the subgroups are mixed for a discussion, is that there is a sharp distinction in modern aquatic excosystems in form and dynamics between ultra and microplankton (Fogg, 1995), and we can supposed it is also true for the fossil record.

In the Mesozoic, the smallest elements are described by Habib and Knapp, with *Claviticystis bulbis* (4.1 µm to 8.5 µm in total diameter), *Conaticystis orbis* (4.88 µm to 6.22 µm), the *Nannobarbophora* spp. (6.9 µm to 13.6 µm), *Tabulimicrocystis tetragonis* (4.3 µm to 8.5 µm), *Verrucidium globosum* (4.5 µm to 6.98 µm), or *Cymatiosphaeropsis rotundus* (4.9 µm to 15.5 µm)

Other species such as *Lecithodinium ciliatum*, in the same work, have a very large dispersion of size, between 9 to 48 µm in total diameter.

These small acritarchs demonstrate their stratigraphic utility in the Cretaceous (Habib and Knapp, 1982), but also the Neogene (e.g. de Vernal and Mudie, 1989; Head, 2003). In QSIM 801 material, the disctinctive morphology of *Micrhystridium regulum* nov. sp., and its distribution, shows a good potential as biostratigraphical marker in the late early to late Darriwilian.

Clusters of minute palynomorphs

The last category of minute palynomorphs but the second group in terms of importance, consist of clusters and aggregates of sphaeromorphs. These elements, with cells of small size, between 5 µm and 25 µm are particularly abundant in the Saq Formation (up to 40% of the palynomorph content) but are also reccurent and abundant in several levels of the Hanadir member.

The clusters can be loosely packed units, with elements close together but no really adherent, and smooth or ornamented. They are clusters of Type 1. Many of these clusters, or irregular aggregations, found in the Proterozoic, with some equivalent in the QSIM material, are frequently described as *Symplassosphaeridium* spp., or *Synsphaeridium* spp. (cf. e.g. Reidman et al., Figs. G, H, S, P and U; Wellman and Strother, 2015, Fig. 2, H. or Baludikay et al., 2016, Fig. 12, M). But it can be noted that descriptions of the two genera are quite ambiguous, and *Synsphaeridium* was

rejected by Loeblich and Tappan, 1976, on the reason that its type species is also the type species of *Protoleiosphaeridium* (= *Leiosphaeridia*). We consider that many of these irregular aggregations correspond probably to clusters small prasinophycean phycomata, of leiospheres type. Someones, with pseudoreticulate ornamentation and small rounded openings (Plate 7, Fig. 19) recall spores of chlorococcales, such as the cell clusters of spores of *Palambages morulosa* illustrated by Tappan (1980, Fig. 10.25, p. 837).

Arrangements are also found in dense packings with units close together. They are clusters of Type 2, that form structures comparable to cryptospores masses (particularly Pl. 7, figs 17, 18, 20) such as the fragments of sporangium illustrated in the Ordovician of Oman (Wellman et al., 2003). We do not have found in the material of QSIM-801, the regular and planar arrangement of the cryptospore clusters described in the Middle Ordovician of Utah (Vecoli and Strother, 2016).

With the frequency and the diversity of cryptospores in the residues of QSIM-801 of Dapingian(?) to late Darriwilian age (Steemans et al., this volume), the existence of others fragments of this phase of vegetation, and possibly of miniscule plants like in Oman, is a possibility, even thought the interpretation will remains controversial without more detailed morphological analysis of the elements of the clusters.

Discussion

The occurrence of minute palynomorphs in the Middle Ordovican from Saudi Arabia, do not correspond to a drastic reduction of body size of the microfossils. They are not attributed to a “Lilliput Effect“(Urbanek, 1993), because not all the elements of the microfloras tend to be much smaller than elements in the preceding levels. In the same way, because large microfossils, such as *Aremoricanium rigaudae* or *Tyrannus proteus* etc., are present before and after deposition of the Hanadir Shales, the small size of a part of the microfossils is not due to hydrodynamic sorting.

It is important to recognize, after Riegel et al. (2014), that small acritarchs form a unique segment of microphytoplancton assemblages, which appear abundant only in special environments and at certain stratigraphic levels. Some equivalents of assemblages with small acritarchs, as described in the Mesozoic are also known in the Paleozoic, in specific intervals of time and in specific environments. For the

Ordovician, the abundance of minute acritarchs recorded in the middle Ordovician of Saudi Arabia, seems at this moment exceptional and suggests an adaptation ot this fraction of palynomorphs, particularly the smallest ones, to special conditions in that interval of time.

The abundances of small acanthomorphs (in majority *Micrhystridium* spp.) are variously interpreted in the literature.

Schrank (2003) suggests an adaptation of the small acritarchs found in sands of the upper Cretaceous of Egypt to an interstitial mode of life. This relationship between acritarchs and coarse-grained littoral sediments have been also previously suggested by Courtinat (2000) or Sarjeant and Taylor (1999), but as noted by Riegel et al (2014), it is not consistent with the occurrence of minute acritarchs and prasinophytes in oceanic clays and marls of the Lower Cretaceous of the western North Atlantic (Habib and Knapp, 1982), nor in limestones and marls of the Middle Triassic Jena Formation they studied in Germany. The conclusions of Riegel et al., are there is no single mode of life for the small acritarchs, but for their Triassic record they mainly proposed the proportions are essentially salinity controlled.

With other indices, the high polymorphism for several species, the variations in terrestrial input (e.g. cryptospores abundances and clusters of possible cryptospores masses etc.), we also suggest that changing salinity may explain the frequent changes in the palynomorph assemblages, and the abundance of minute palynomorphs.

3.1. Biozonation and comparisons

Among the acritarchs and prasinophycean phycomata of QSIM-801 assemblages, the presence of *Arkonia* spp., *Frankea* spp. or *Striatotheca* spp., clearly indicate affinities with the temperate to cold Mediterranean Province or Perigondwana Province (Molyneux et al., 2013). These genera are not known in the Baltic province. If there is no simple relationship between acritarch biogeography, the paleolatitudes and climate, as postulated by Molyneux et al. (2013), nevertheless, the distribution of some genera such as *Frankea* could suggest they occupy latitudinally distinct temperature defined water masses (Rubinstein et al., 2011), and relatively high

paleolatitudes (Colbath, 1990), even though in Saudi Arabia it will be the most northerly occurrence of the genus.

The vertical distribution of acritarchs and prasinophycean phycomata (Table.1) revealed significant fluctuations within palynomorph assemblages. Precisions on that are provided through detailed counts, and variations in relative abundance of taxa and palynomorph groups (Table 2).

The sequence of Saq/Hanadir transitional beds in QSIM-801, is divided into 3 major intervals, the Assemblages Zones 1 to 3, with assemblage Zone 3 subdivided, characterized by different assemblages of acritarchs and prasinophycean phycomata. The changes in the composition of assemblages of marine palynomorphs, and the biostratigraphic events detected in the section, which include lowest (LAD) or highest (FAD) occurrences, acme events etc., are certainly partially controlled by local environmental conditions. Some inconsistencies in the stratigraphical ranges of important taxa, known elsewhere, may be also explain by reworking.

Only the taxa which are useful for the identification of each zone or subzone are cited. Many accessory forms are present, but without direct biostratigraphic value.

Assemblage Zone 1

The lowermost assemblage from the deepest core samples of core 8 in the Saq Formation (from 767.8 to 762.3 ft.) shows a predominance of prasinophytes represented by leiospheres of variable diameter, some clusters of small sphaeromorphs and some enigmatic striate sphaeromorphs. There is only a little diversity of acritarchs, and the chitinozoa are poorly represented. Among the acritarchs are *Aremoricanium rigaudae* (rare), *Arkonia* sp. A, *Aureotesta clathrata*, *Dicrodiacrodium ancoriforme*, *Comasphaeridium* aff. *C. piluliferum*, *Frankea breviuscula*, *F. longiuscula*, some galeates, *Michystridium* spp., *Polygonium* spp., *Stellechinatum celestum*, and few veryhachids. The cryptospores, which are allochtonous elements introduced into the marine assemblage, count for 3 to 6,5% of the total palynomorphs. This relatively high abundance of cryptospores associated to poor representativity of chitinozoa and low diversity of acritarchs, is consistent with the characteristics of the deposits: some tidal sand flats in a marginal marine

environment (shallow shelf-sea). The enigmatic grey elements (cf. discussion above) are present, and they will continue more or less abundant all along the section.

The *Leiosphaeridia* spp. are major components of the assemblages. They consist of separate individuals up to 100 µm in diameter, or clusters, that represent respectively between 43 to 76 %, and 19 to 42.6% of the assemblages. They continue to be important in the assemblage Zone 2 above, in the bedded sandstones up to 754.8 feet, where they represent 81.85% of all the palynomorphs. They are still abundant with high percentages, in the assemblage Zone 3, in the rest of the section. The importance of the *Leiosphaeridia* spp. is a characteristic of the Saq/Hanadir transitional beds. A comparison can be proposed with the Oligocene, where the dominance of these forms is considered as a climatic signal. High numbers of leiosphaerids are recorded for example from glacio-eustatic sedimentary cycles, in ice marginal environments under seasonal ice and in low salinity and temperature environments in circum-artic and Antarctica (Mudie, 1992, Prebble et al. 2006). In the Triassic of North China it has been demonstrated a correlation between highly abundant oil-prone leiosphaerid acritarchs and hydrocarbon source rocks (Ji et al., 2008). In the Saq/Hanadir sequences, the unusual abundance of these sphaeromorphs, isolated or in colonies, and some of them possibly of freshwater origin, could be a major contributor of the highly mature type II kerogen and TOC values, between 0.5 to 2.98% registered in the Hanadir shales member (Ghazwani, 2012). The striate sphaeromorphs, previously illustrated as Hilate sporomorph 1 (in Le Hérissé et al., 2007), and *Cymatiosphaera* sp., first appearing in this biozone, but that continue in biozones 2 and 3, are also reported from the Saih Nihayda Formation of Mid to Late Darriwilian in Oman (Rickards et al., 2010, Plate 2, respectively Figs. m and o as spore indet. B, and Fig. d as Incertae sedis N°20).

The genera *Dicrodiacrodium* and *Frankea,* present in this lowest assemblage, have a FAD in the late Arenig (Brocke et al., 1995), in an interval attributed now to the Dapingian (Li et al., 2010). In our material *Frankea breviuscula* and *Frankea longiuscula* (rare) are represented. The last one is more abundant in the assemblage Zone 3, particularly with the polymorph *F. longiuscula* var. *darriwilense* nov. var. The species *F. longiuscula* is normally considered indicative of a middle Darriwilian or younger age (Vecoli & Le Hérissé, 2004). The assemblage Zone 1 is also characterized by the first appearance of *Arkonia*, with *Arkonia s*p. A, a species

described in the Rhadames Basin in North Africa (Vecoli, 1999). According to Servais (1997), the first occurrence of *Arkonia* corresponds to the British *D. hirundo* graptolite Zone, of latest Arenig age, i.e. early Darriwilian, and equivalent of the *U. austrodentatus* zone of South China (Yin et al., 1998). *Aureotesta clathrata* is reported from many “Arenig-Llanvirn” sections all over the world (Li et al., 2010), and if FAD of the species is important stratigraphically, its occurrence there is not so significative. With these first results the age Dapingian of this part of the uppermost Saq Formation is in question. It can be mentioned also that the *Desmochitina ornensis* Zone of chitinozoa has not been seen in this section. It could be suggested a possible early Darriwilian age for the interval, as an equivalent of the *bulla* event of chitinozoa, sometimes registered locally in the upper part of the Saq Formation (Paris, unpublished data; Paris et al., 2007).

Assemblage Zone 2

Zone 2 holds parts of core 8 and 7, from 759.6 to 754.8 (included). The marked increase in the relative abundance of chitinozoa (from an average of 1,63% top of Zone 1 to an average of 21,5 %, base of zone 2), and in the diversity of acritarchs, indicates that rapid marine flooding of the site occurred between 762,3 and 759,6 ft.. This is consistent with the drop of diversity of cryptospores (1,88 %). The sedimentary structures of cross stratification suggest tidally influenced environments, and it is possible that the flooding is underlined by an unconformity between these depths. The interval marks the introduction of *Siphonochitina formosa* among the chitinozoa, and among the acritarchs the range base of the genus *Striatotheca,* with introduction of *S. rarirrugulata,* the presence of *S. monorugulata* and *S. mutua* confined to the zone, of *Acanthodiacrodium costatum*, *Ampullula suetica* (uncommon), *Ankyrotrochos crispum, Micrhystridium regulum* nov. sp., *Pteospermopsis colbathii*, *Tyrannus proteus* nov. sp., *Uncinisphaera fusticula*, and last occurrence of *Arkonia* sp. A and *Aureotesta clathrata*, at the end of the zone. These disapearances to the boundary between zone 2 and 3 could indicates a possible environmental control on the distribution of these species, that normally are know to be extended higher elsewhere.

We have noticed the introduction, in this assemblage zone, of minute acritarchs and small sphaeromorphs of ultraplanctonic size, between 5 to 15 µm, but in low proportions compared to the the interval of Zone 3 above.

The FAD of *Tyrannus proteus* named *Tyrannus* sp. A in Le Hérissé et al. (2007), has been precised and is in top of core 8. This enigmatic form, very polymorph, recurrent but intermittent into the rest of the section from 759.6 ft., is interesting because it is also known in others core sections of the middle Ordovician in Saudi Arabia (e.g. Turabah-1 well).

The assemblage of this second zone, referred to the uppermost Saq Formation, is more characterisitic of the Darriwilian than the Dapingian, based on comparisons with other localities of the Northern Gondwana Domain. For example *Striatotheca monorugulata* is interesting since the species is considered to have a short range which extends not above the late *D. hirundo* graptolite zone and equivalents, e.g. the *U. austrodentatus* zone of South China (Yin et al., 1998), i.e the early Darriwilian. Other taxa such as *Ankyrotrochos crispum* or *Pterospermopsis colbathii* are not reported elsewhere in deposits older than the Darriwilian (Vecoli and Le Hérissé, 2004).

Some taxa such as *Caldariola glabra* (rare) could be reworked from underlying strata, and if a mid Darriwilian age is confirmed by the occurrence of *Siphonochitina formosa*, it could be considered that *Striatotheca monorugulata*, normally not found above the early Darriwilian, is also possibly reworked. It can be mentioned that Al Hajri (1995, p.33), studying chitinozoa was also previously speaking of possible extensive “Arenig” reworking of the Saq Formation into the “Llanvirn” Hanadir Member at the base of the Qasim Formation.

Assemblage Zone 3

From 751.8 ft., a level taken as the limit Saq/Hanadir on sedimentological arguments, samples proved much productive, with introduction of several species of importance, in two successive intervals: from 751.8 ft to 715.6 ft, Zone 3A; from 712.7 to 675.1 ft., Zone 3B.

To 751.8 ft., the palynofacies analysis reveals also a significant increase in relative proportion of amorphous organic matter, with percentages of 30 % of all organic

elements at 751.8 ft. compared to only 15% at 754.8 ft. This sudden accumulation of organic matter can be interpreted as a clear deepening of the sequence in the Hanadir shales, but also could indicate a discontinuity.

The assemblage Zone 3A is dated by chitinozoa to the *formosa* Biozone, and the assemblage Zone 3B concerns top of the *formosa* Biozone and continues in the *pissotensis* Biozone from 699.9 feet.

Several groups of acritarchs are abundant in Zone 3: the galeates, the *Baltisphaeridium* spp., the *Micrhystridium* spp., the *Veryhachium* spp., and one species, *Frankea longiuscula* var *darriwilense* nov. var., which appears over-represented, compared to the other taxa.

Micrhystridium regulum nov. sp., which first appears in Zone 2, but is more represented in Zone 3, is potentially of interest regionally as biostratigraphic marker, in spite of its small size.

The Zone 3A shows progressively the introduction of *Baltisphaeridium klabavense, B. ternatum, Dasydorus cirritus, Peteinosphaeridium trifurcatum, Barakella fortunata, Striatotheca quieta, Vogtlandia ramificata, Focusphaera elongata, Barakella rara* and *Peteinosphaeridium velatum*, among the most important species.

The *Aremoricanium* spp. are also represented with *Aremoricanium rigaudae* but that rapidly disappears to only reappear in the Zone 3B, and *Aremoricanium* aff. *A squarrosum* which is a pigmented cyst.

Focusphaera elongata (mis-identified as *Tinacula* sp. in Le Hérissé et al., 2007), has been previously described in the Middle Ordovician of the Solimões Basin, Benjamin Constant, Brazil by Quadros (1986a), in the local Arkonia virgata zone, dated Arenig-Llanvirn (Quadros, 1988).

Zone 3A shows also the highest percentages of AOM (kerogen), in a range depth between 751.8 and 739.3 ft. They probably indicate the more distal basin-floor sediments of the succession.

Another significant change in distribution of the acritarchs, that seems to be of chronostratigraphical value, appears to occur at the level 728.5 ft. We propose a tentative limit of Biozone 3 at this level, distinguishing a sub-zone 3B, with

introduction of *Poikilofusa ciliaris*, *Pterospermopsis franciniae, Vogtlandia tenuata*, *Aremoricanium* aff*. A. decoratum,* and successively *Vogtlandia* sp. A in Vecoli, 1999, *Glaucotesta latiramosa*, *Striatotheca principalis parva*, *Dactylofusa striatogranulata*, *Acanthodiacrodium uniforme*, *Striatotheca frequens*, *Frankea sartbernardensis*, and the first *Orthosphaeridium* etc.

We encountered only one specimen of *Barakella felix* at 728.5 ft., at the base of Zone 3B. Because the species is normally restricted to the Arenig, it is possibly reworked in our material, or indicates its upper stratigraphic range might be younger in Saudi Arabia than elsewhere.

The limit between the subzones 3A andf 3B corresponds also to the LAD of *Ankyrotrochos crispum.*

Two discontinuities are indicated by the sedimentology in Zone 3B, at 697.5ft. and 705.7 ft., that seems to be marked by changes in the assemblages, e.g. by LAD of *Barakella rara*, *S. principalis parva*, *S. frequens* at 697.7 ft, FAD of *?Dorsenidium* sp., *A. uniforme* at 704.3, of *M.* aff. *multipugiunculatum* at 695.7ft, and reappearance of *A. rigaudae* at 695.7 ft.

The assemblages of Zone 3 show similarities with assemblages described in Tunisia (Vecoli, 1999; Vecoli et al., 1999), in the *Frankea sartbernardensis-V. ramificata* zone attributed to the Llanvirn (Mid to Late Darriwilian). But there are notable anomalies between the two areas, because the species that globally appears in the same level in Tunisia, appears more progressively in Saudi Arabia. It is difficult to resolve these differences that might be accounted for paleogeographical situation, for by ecological controls exerted on the composition of the assemblages or are reflection of possible disconformity in the Darriwilian in Tunisia compared to Saudi Arabia, with the Llanvirnian Bir ben Tartar Formation directly on the Tremadocian Sanrhar Formation.

It can be noted that *F. sartbernadensis*, a classical marker of the upper Arenig to Llanvirn (Darriwilian) elsewhere (Vecoli and Le Hérissé, 2004), is very rare in the material of QSIM 801, and appear only in an equivalent of the late Darriwilian. It seems that facies control strongly influenced the stratigraphical distribution of this species.

Many species of assemblage Zone 3 are also common with the Medditeranean-type assemblage recorded in Spain by Albani (in Guttierez Marco et al., 1996), in an equivalent of the *Linochitina psissotensis* Zone, with similarly some Baltic elements such as *Peteinosphaeridium bergstoemii* and *P. velatum* (see discussion in Tongiorgi and Di Milia, 1999). Comparable assemblages have also been recorded from the Llanvirnian of Jordan, in the Zone JO-3 of Keegan et al. (1990), but without precisions about the succession of the species.

Pterospermopsis franciniae and *Dactylofusa striatogranulata* have been previously described in the Llanvirnian (but not basal) *Aremoricanium solaris* and *Dactylofusa striatogranulata* Zones of Goldwyer and Tina Formations in Australia (Playford and Martin, 1984, Hashemi and Playford, 2006), a distribution consistent with the distribution herein.

Many species are common with the Middle Ordovician (Llanvirn) of Bohemia, and we mentioned for the first time in Saudi Arabia, *Glaucotesta latiramosa*, previously described in the Sarka Formation, in the Llanvirn (Vavrdova, 1982).

3.2. Relative abundances variability

Table 2 and 3 show the variations of relative abundances of acritarchs, of other palynomorphs both marine and continental, and of the amount of amorphic organic matter in the QSIM-801 borehole. These data indicate that the Saq/Hanadir transition in QSIM-801, and the Hanadir member, know important events which are reflected in a series of complex responses in the distribution of the palynomorphs and abrupt and rapid changes in the compositon and percentages of acritarchs and associated groups.

Advantage of this sequence to the Saq/Hanadir transition is that it represent quite continuous sedimentation (with exception of the discontinuities), with the chitinozoan biostratigraphy that provide a good temporal constraint. It is dated from the beginning of the *formosa* zone up to the beginning of the *pissotensis* zone and higher, i.e with problem of a questionable late Dapingian to the bottom, major part of the Darriwilian from 759.6 ft. With an estimated duration of the Darriwilian at c 9 My (Cohen et al., 2013), the QSIM 801 section is very condensed, 93 ft. compared for example with the Middle Ordovician in the Armorican Massif, in a coeval interval (*formosa* zone to the

beginning of the *pissotensis* zone), that consists of several hundreds of meters (Dabard et al., 2015).

The most important taxonomic categories and species, that exhibit relatively high frequencies are: the galeates, *Frankea longiuscula* var. darriwilense, the leiospheres, the *Micrhystridium* spp., the *Veryhachium* triapsidate, the chitinozoa, the cryptospores and the clusters of sphaeromorphs. Among the different taxa, some can be frequent such as *Uncinisphaera fusticula* from Assemblage Zone 3, or *Tyrannus proteus*, and the *Stellechinatum* spp. in the upper part of the section.

The introduction of the two chitinozoa *Siphonochitina formosa* and *Linochitina pissotensis* respectively at 759.6 ft and 699.9 ft. (with the data in hand actually), marks two transgressive events, consistent in our quantitative analysis for example by the introduction of new species (e.g. *A. clathrata*, the *Arkonia* etc.), or the drop in the representativity of the cryptospores. The wide distribution of these events on the north gondwanan margin and the middle east, their amplitude and rapidity, exclude they are of tectonic origin, but are of glacio-eustatic origin (Dabard et al., 2015, p. 107). These sea-level rise surfaces are accompanied for the main groups of palynomorphs cited above by very rapid fluctuations of frequencies that could be related to rapid se-level fluctuations.

The limit between assemblages zones 2 and 3, at 751.8 ft is also well marked by a significant increase in the frequencies of galeates, of *Micrhystridium* and *Veryhachium* but also of *Baltisphaeridium*, *F. longisucula* var. *darriwilense*, and *Uncinisphaera fusticula,* This limit shows also an important peak of amorphous organic matter.

The ratio between the cryptospores (terrestrially-derived or coastal elements) and the *Michystridium* spp. are globally inversely proportional. We have globally an inverse relationship also between abundances of leiospheres and of some species over-represented such as *Frankea longiuscula* var. *darriwilense*. Absence or quasi-absence of the last species globally between 754.8 and 567.8 ft. is compensated with high frequencies of leisopheres, that could be indicator of restricted conditions, consistent with the facies of tidal siltstones and subtidal sand flats, and good percentages of cryptospores. A response, quite equivalent, is registered between 685.9 ft and 687.2 ft, with low percentages of *F. longiuscula* var. *darriwilense*, of

galeates, absence or low percentages of *Micrhystidium* spp., but good proportions of Leiospheres and also cryptospores (with the most important frequencies 6.73 up to 8,7%). Abnormal quantity of cryptopsores, capable of diluting many other marine palynomorph, with exception of the pelagic chitinozoa, will indicate the vicinity of active fluvio-deltaic sources (Tyson, 1993). Changes in the palynomorph associations are certainly controlled by salinity changes, influenced by sea level fluctuations, and as responses to pulses of delta advance or retreat. We have suggested previously, taking hypothesis of work in the Mesozoic (Riegel et al., 2016), that fluctuations in abundance of minute palynomorphs, could indicate conditions of changing salinity. Occurrence of important polymorphism of some species, *F. longiuscula* var. *darriwilense*, *D. ancoriforme* or *T. proteus*, but also presence regularly of aberrant forms (AA), will indicate, by comparison to dinoflagellates (e.g. Ellegaard, 2000), conditions of changing salinity in the Hanadir member.

The appearance of reasonably diverse cryptospore assemblages in the Middle Ordovician Saq Formation and Hanadir Member of the Qasim Formations (Strother et al., 2015; Steemans et al., this volume), and clusters comparable to cryptospores masses (possible fragments of sporangia?) requires some considerations, as evidence of a major stepwise and relatively rapid adaptation of plants at this time. It is know that changes in vegetation cover amplify the orbitally driven temperature variations (Horton et al., 2010; Pohl et al., 2016), with impact on the climate, on the silicate weathering and atmospheric CO_2 (Strother at al., 2010; Young el al., 2010; Le Hir et al., 2011; Lenton et al., 2012) and have incidence on glacial-interglacial fluctuations. But surprisingly, when terrestrialization steps have major consequences for the carbon cycle and climate cooling, for several intervals in the Paleozoic (Kenrick et al., 2015), at that time the effects of middle Ordovician vegetation phase seem not tenable (Pohl et al., 2016).

The *Micrhystridium* (Tabl.2 and 3) show rapid changes in frequencies, all the 1 to 4 meters. The most stricking changes are close to the limit Saq/Hanadir, placed in sedimentologic arguments, between 754.8 and 751.8 ft. (respectively 2,4 and 31 %), which is also the limit between Zone 2 and 3A, and between 731.6 and 728.5 ft. (respectively 10.52 and 32,52 ft.), that corresponds also to the limit between Zone 3A and 3B. At 728.5 we have the maximum of diversity recorded among the acritarchs, which could correspond to a maximum flooding surface. At 751.8 ft, with the

presence of reworking (see biostratigraphy), we have may be an episode of erosion and redeposition which is likely to have incorporated material from older strata into younger.

The variations of *Micrhystridium* abundances seem to be also useful to identify discontinuities. Two examples of discontinuities have been recognized by sedimentologists: a first one at 697.5 ft, where a conglomeratic lag deposit indicates from top to the bottom a transition between distal prodelta facies and proximal prodelta facies; a second at 705.7 ft but more difficult to interpret.

In the first case there is an abrupt change in the frequencies of the *Micrhystridium*, from the more marine conditions, 10,4% at 695,7, to only 2.3 % at 697.7 in more restricted conditions. The second discontinuity shows the inverse, very low percentages, 0.58% at 704.3 ft and high percentages, 15.1 % at 712.7 ft, but the results are not so significative than for the preceding example taking account of the distance between our samples. Other elements of the quantitative analysis confirm the tendencies, for example in the first discontinuity, with no representation of the cryptospores in the distal prodelta facies (0%), but quite good representativity in the proximal pro-delta facies (2.3%).

The group of triapsidate acritarchs, of the genera *Arkonia, Frankea* and *Veryhachium*, is well represented, and we have also the development of triangular variants of *Tyrannus proteus*, The percentages of the triapsidate *Veryhachium* in the Hanadir shales, attain for example 13 to 20% of all the palynomorphs in several samples. We have previously suggested they indicate a possible climatic deterioration and cooling (Le Hérissé et al., 2007, p.12), by comparison with the situation we know associated with the late Ordovician glaciation.

Another element important to be discuss is the presence of abnormal forms of acritarchs (AA on the Tabl. 2), in several samples of the Hanadir shales. We have few measures of δ13C, but a clear excursion in the Hanadir Shales. Other occurrences in the Early Paleozoic are associated to D13C excursions and specific environmental circumstances (Munnecke et al., 2012). We have also D13C excursion in the QSIM-801 well (Fig. 6) but not with the same amplitude than in the Hirnantian or Silurian according to Kaljo et al. (1995) and Sheehan (2001). We Nhave to confirm the isotopic excursions in the Middle Ordovician of Saudi Arabia, by more important

analysis. In the discussion by Munnecke et al. (2012), the other finding is that many occurrence of teratological acritarchs appear around a glacial event. These results on the QSIM-801 material allow to suggest a new time slice in the Early Paleozoic with malformed acritarchs, as indicator of environmental changes, possibly with the onset of a glaciation (?).

Question is to be certain or not if the mechanism of these changes in the palynomorph abundances, in the Saq/Hanadir transition and in the Hanadir, can be explain by glacio-eustasy, as proposed in the Armorican massif or Jordan (Dabard et al., 2016; Turner et al., 2012) using high frequency eustatic sea-level changes during the Middle to late Ordovician. Question is to consider if palynological informations, as analysis of the genetic units, can provide indirect evidence for a Darriwilian Ice Age in Gondwana.

Conclusions

- The biostratigraphic framework for this study (on a short but continuous section well sampled), based on chitinozoa and acritarchs and prasinophycean phycomata assemblages, provides essential age constraints to date locally the Saq/Hanadir transition.
- The biological significance and the classification of problematic microfossils can be aided by the use of CLSM and the variations of intensity of fluorescence signals.
- Detailed quantitative analysis reveals high frequency variations and abrupt changes in the distribution of marine and non-marine palynomorphs, as possible evidence of third-order cyclicity. The analysis confirm also the importance of the triapsidate acritarchs and the frequency of abnormal forms that could suggest an environmental stress and possibly a glacial event.
  Of particular interest will be to study in parallel the isotopic trends ($\delta^{13}C$, $\delta^{18}O$, $\delta 15N$), the eustatic sea-level changes and palynomorph assemblages to establish a formal link between them.
- The *Frankea longiuscula* var. *darriwilense* acme and its extreme polymorphism, associated to minute palynomorphs in relation with variations of terrigenous delivery (cryptospore signal), could be indicator of changing salinity during the darriwilian

- The organic richness of samples, particularly in the Hanadir Shales Member is related to mixed terrestrial organic productivity and marine aquatic organic productivity, and to the extension of anoxic conditions. These elements permitted an increase in the organic matter deposition and good TOC values
- The good proportion of minute palynomorphs compared to other parts of the Paleozoic, may indicates a locally severe ecological effect of the environmental changes on the composition of palynomorph assemblages (controlled by salinity?, or climate-driven?).
- Although these results must be regarded as provisional, they suggest that high-resolution quantitative palynological studies, can provided a good tool for the identification of eustatic signatures, but also for changing salinity in the Middle Ordovician. Our findings and signals provided by the study of palynomorph assemblages add significant support for recent studies that have argued for the presence of ice sheets since the Middle Ordovician Darriwilian.

Disclosure of interest

The authors report they have no potential conflict of interest.

Acknowledgements

We acknowledge the Saudi Arabian Ministry of Petroleum and Mineral Resources and the Saudi Arabian Oil Company (Saudi Aramco) for providing the material for study and permission to publish. This study is a contribution to the programme “Nano”, granting by the Labex Mer of University of Brest and IUEM. We thanks Pierre Sanjoffre of Geosciences Océan laboratory for isotopic analysis and PIMM-DRX Imagery platform of University of Brest and Gérard Sinquin and Phillipe Elies for their assistance in the CLSM and SEM studies.

We also aprreciate the constructive comments of …. Which have allowed us to improve the manuscript.

Bibliography

Agic, H., 2015. A new species of small acritarchs with a porous wall structure from the early Cambrian of Estonia and implications for the fossil record of eukaryotic picoplankton. Palynology, 2015. 1-14.

Albani, R., Bagnoli, G., Ribecai, C., Raevskaya, E., 2007. Late Cambrian acritarch *Lusatia*: Taxonomy, palaeogeography and biostratigraphic implications. Acta Palaeontologica Polonica, 52, 4, 809-818.

Al-Hajri, S., 1995. Biostratigraphy of the Ordovician chitinozoa of northwestern Saudi Arabia. Review of Palaeobotany and Palynology 89, 27-48.

Baludikay, B.K., Storme, J.-Y., François, C, Baudet, D., Javaux, E.J., 2016. A diverse and exquisitely preserved organic-walled microfossil assemblage from the Meso-Neoproterozoic Mbuji-Mayi Supergroup (Democratic Republic of Congo) and implications for Proterozoic biostratigraphy. Precambrian Research, 281, 166-184.

Barber, R.T., Hilting, A.K., 2002. Histrory of the study of plankton productivity. In: Phytoplankton productivity – Carbon assimilation in marine and freshwater ecosystems. Williams P.J, Thomas, D.N, Reynolds, C.S. (Eds), Blackwell Science, 16-43.

Borjigin, T., Yin, L., Yuan, X., Zhou, C., Meng, F., Xie, X., Bao, F., 2014. Nanoscale spheroids and fossils from the Ediacaran Doushantuo Formation in China. The Open Paleontology Journal, 5, 1-9.

Brocke, R., Riegel, W., 1996. Phytoplankton responses to shoreline fluctuations in the Upper Muschelkalk (Middle Triassic) of Lower Saxony (Germany). Neueus Jahrburg für Geologie und Paläontologie, Abhandlungen, 200, 53-73.

Brocke, R., Fatka, O., Molyneux, S.G., Servais, T., 1995. First appearance of selected Early Ordovician Acritarch taxa from peri-Gondwana. In Coop, J.D., Droser, M.L. & Finney, S.C. (eds.), Ordovician Odyssey. The Pacific Section for Sedimentary Geology, 77: 473-476.

Burmann, G., 1970. Weitere organische Mikrofossilien aus dem unteren Ordovizium: Paläont. Abh., B, Paläobot., 3, ¾, 289-332.

Butterfield, N.J., 2009. Modes of pre-Ediacaran multicellularity. Precambrian Research, 173, 201-211.

Butterfield, N.J., Knoll, A.H., Swett, K., 1994. Paleobiology of the Neoproterozoic Svanbergfjellet Formation, Spitsbergen. Fossils and Strat, 34, 1-84.

Cohen, K.M, Finney, S.M., Gibbard, P.L., Fan, J.-X., 2013. The ICS International Chronostratigraphic Chart. Episodes, 36 (3), 199-204.

Colbath, G.K., 1986. The lower Paleozoic organic-walled phytoplankton (“acritarch”) genus *Frankea* Burmann, 1970: Micropaleontology, 32, 1, 72-73.

Colbath, G.K., 1990a. Palaeobiogeography of Middle Paleozoic organic-walled phytoplankton. In: Mc Kerrow, W.S. and Scotese, C.R. (eds.). Palaeozoic Palaeogeography and Biogeography. Geological Society, London, Memoirs, 12, 207-213;

Cooper, A.H., Fortey, N.J., Hughes, R.A., Molyneux, S.G., Moore, R.M., Rushton, A.W.A., Stone, P., 2004. *The Skiddaw Group of the English Lake District*. Memoir of the British Geological Survey (England and Wales), Parts of sheet 22, 23, 24, 28, 29, 30, 31 and 48.

Courtinat, B., 1983. Evidence ou réalité chez le genre *Micrhystridium*. Un exemple par l’étude des quelques formes Jurassiques du Jura Français. Cahiers de Micropaléontologie, 1, 1-32.

Cramer, F.H. and Díez, M.D.C., 1977. Late Arenigian (Ordovician) acritarchs from Cis-Saharan Morocco. Micropaleontology, 23 (3), 339-360.

Dabard, M.P., Loi, A., Paris, F., Ghienne, J.F., Pistis, M., Vidal, M., 2015. Sea-level curve for the Middle to early Late Ordovician in the Armorican Massif (western France) : Icehouse third-order glaciaoeustatic cycles, 436, 96-111.

Davies, N.S, Gibling, M.R., 2010. Cambrian to Devonian evolution of alluvial systems: the sedimentological impact of the earliest land plants. Earth Science Reviews 98 : 171-200.

De Vernal, A., Mudie, P.J., 1989. Pliocene and Pleistocene palynostratigraphy at ODP Sites 646 and 647, eastern and southern Labrador Sea. In S.P. Srivastava, M.

Arthur, B. Clement et al. (eds.). Proceedings of the Ocean Drilling Program, Scientific Results, 105. Ocean Drilling Program, College Station, Texas, 401-402.

El-Khayal, A.A., Romano, M., 1988. A revision of the upper part of the Saq Formation and Hanadir Shales (Lower Ordovician) of Saudi Arabia. Geological magazine, 125, 161-174.

Ellegaard, M., 2000. Variation in dinoflagellate cyst maorphology under condition of changing salinity during the last 2000 years in the Limfjord, Denmark. Review of palaeobotany and palynology, 109, 65-81.

Fatka, O., Molyneux, S.G., Servais , T., 1996. The Ordovician acritarch Frankea: some criticals remarks. Geobios, 30, 321-326.

Feist-Burkhardt, S., Pross, J., 1999. Morphological analysis and description of Middle Jurassic dinoflagellate cyst marker species using confocal laser scanning microscopy, digital optical microscopy and conventional light microscopy. Bull. Centr. Rech. Explor. Prod. Elf Aquitaine, 22, 1, 103-145.

Feist-Burkhardt, S., Götz, A., Ruckwied, K., Russell, J.W., 2008. Palynofacies patterns, acritarch divetrsity and stabe isotope signatures in the Lower Muschelkalk (Middle Triassic) of N Switzerland: Evidence of Third-order cyclicity. Swiss J. Geosci., 101, 1-15.

Fogg, G.E., 1995. Some comments on picoplankton and its importance in the pelagic ecosystem. Aquatic microbial ecology, vol. 9., 33-39.

Ghavidel-Syooki, M., Popov, L.E., Javier Alvaro, J., Ghobadi Pour, M., Tolmacheva, T.Y., Eshani, M-H., 2014. Dapingian-Lower Darriwilian (Ordovician) stratigraphic gap in the Faraghan Mountains, Zagros Ranges, southeastern Iran. Bulletin of Geosciences, 89, 4, 679-706.

Ghazwani, A.H., 2012. Investigation of source rock potential and micropaleontology of the Middle Ordovician Hanadir Member of the Qasim Formation, Northwestern Saudi Arabia. 167p.

Ghienne, J.-F., Le Heron, D.P., Pollard, D., Levy, R.H., 2016 . The Late Ordovician glacial sedimentary system of the North Gondwana platform. In Glacial Sedimentary

Processes and Products, Spec. Publ. Int. Assoc. of Sedimentologists, M. Hambrey et al. (eds.) Blackwells, Oxford, U.K., 295-319.

Götz, A.E., Feist-Burkhardt, S., 2012. Phytoplankton associations of the Anisian Peri-Tethys Basin (Central Europe): Evidence of basin evolution and paleoenvironmental change. Palaeogeography, Palaeoclimatology, Palaeoecology, 337-338, 151-158.

Gutiérrez-Marco, J.C., Albani, R., Aramburu, C., Arbizu, M., Babin, C., Garcia-Ramos, C., Mendez-Bedia, I., Rabano, I., Truyols, J., Vannier, J., Villas, E., 1996. Bioestratigrafía de la Formación Pizzaras del Sueve (Ordovícico Medio) en el sector septentrional de la escama de Laviana-Sueve (Zona Cantábrica, Norte de España): Rev., Esp. Paleont., 11 (1), 48-74.

Gutiérrez-Marco, J.C., Sá, A.A., García-Bellido, D.C., Rábano, I., 2013. The extent of the Middle Ordovician Dapingian Stage in peri-Gondwanan Europe and north Africa: stratigraphic record, biostratigraphic tools and regional chronostratigraphy, GFF, DOI: 10.1080/11035897.2013.865667, 1-5.

Gutiérrez-Marco, J.C., Sá, A.A., García-Bellido, D.C., Rábano, I., 2016. The Bohemo-Iberian regional chronosratigraphical scale for the Ordovician System and paleontological correlations within South Gondwana, Lethaia, DOI : 10.11 11/let.12197.

Habib, D., Knapp, S.D., 1982. Stratigraphic utility of Cretaceous small acritarchs. Micropaleontology, 28, 4, 335-371.

Haq, B.U., Al-Qahtani, A.M., 2005. Phanerozoic cycles of sea-level change on the Arabian Platform. GeoArabia, 10, 2, 127-160.

Head, M.J., 1992. Zygospores of the Zygnemataceae (Division Chlorophyta) and other freshwater algal spores from the uppermost Pliocene St Erth Beds of Corwall, southwestern England. Micropaleontology , 38, 3, 237-260.

Head, M.J., 2003. Neogene occurrences of the marine acritarch genus *Nannobarbophora* Habib and Knapp, 1982 emend., and the new species *N. Gedlii*. J. Paleont., 77 (2), 382-385.

Helal, A.H., 1964. On the occurrence of Lower Paleozoic rocks in Tabuk area, Saudi Arabia. Neues Jahrbuch für Geologie und Paläontologie-Monatshefte, 7, 391-415.

Horton, D.E.C, Poulsen, C.J., Pollard, D. 2010. Influence of high-latitude vegetation feedbacks on late Paleozoic glacial cycles, Nature Geoscience, 3 (8), 572-577.

Ji, L.M., Meng, F.W., Schiffbauer, J.D., Xu, J.L., Yan, K., Shu, J.W., 2008. Correlation betyween highly abundant oil-prone Leiosphaerid acritarchs and hydrocarbon source rocks from the Triassic Yanchang Formation, eastern Gansu Province, Northwestern China, Gondwana Research, 14, 554-560.

Kaljo, D., Martma, T., Männick, P., Viira, v;? éàà"; Implications of Gondwana glacviations in the Baltic late Ordovician and Silurian and a carbon isotopic test of environmental cyclicity. Bulletin de laSociété Géologique de France, 174, 59-66.

Keegan, J.B., Rasul, S.M. and Shaheen, Y., 1990. Palynostratigraphy of the Lower Palaeozoic, Cambrian to Silurian sediments of the Hashemite Kingdom of Jordan. Review of Palaeobotany and Palynology, 66, 167-180.

Kenrick, P., Wellmand, C.H., Schneider, H., Edgecombe, G.D., 2012. A timeline for terrestrialization: consequences for the carbon cycle in the Paleozoic. Phil. Trans. R. Soc., 367, 519-536.

Khalifa, M.A., 1993. Anz Formation: a new Lower Ordovician rock unit, southwest of Al Qasim Province, Saudi Arabia. Egyptian journal of Geology, 37, 53-67.

Khalifa, M.A., 2015. The Ediacaran-Cambrian and Ordovician rocks of Al Qasim Province, Saudi Arabia: facies, depositional history and regional correlation. Journal of African Earth Sciences, 109, 263-282.

Le Hérissé, A., 1989. Acritarches et kystes d'algues Prasinophycées du Silurien de Gotland, Suède. Palaeontographia Italica, 76, 57-302.

Le Hérissé, A., Al-Ruwaili, M., Miller, M., Vecoli, M. 2007. Environmental changes reflected by palynomorphs in the early Middle Ordovician Hanadir Member of the Qasim Formation, Saudi Arabia. Revue de micropaléontologie, v. 50, 3-16.

Le Hérissé, 2015. Ordovician-Devonian acritarch and prasinophyte biostratigraphy of northern and northeastern Brazil. Petrobras project: “Palinologia das Bacias Paleozoicas do Norte do Brasil e Adjacências”. Internal Report, 398p.

Le Hir, G., Donnadieu, Y., Goddéris, Y., Meyer-Berthaud, B., Ramstein, G., Blakey, R.C. 2011. The climate change caused by the land plant invasion in the Devonian. Earth and Planetary Science Letters, 310, 203-212.

Lenton, T.M., Crouch, M., Johnson, Pires, N., Dolan, L., 2012. First plants cooled the Ordovician ; Nature Geoscience, 5, 86-89.

Lepot, K., Compère, P., Gérard,E.,Namsaraev, Z., Verleyen, E., Tavernier, I., , Hodgson, D.A., Vyverman, W., Gilbert, B., Wilmotte, A., Javaux, E.J., 2014. Organic and mineral imprints in fossil photosynthetic mats of an East Antarctic Lake. Geobiology, 12, 424-450.

Li, J., Servais, T., Yan, K., 2010. Acritarch biostratigraphy of the Lower-Middle Ordovician boundary (Dapingian) to the Global Stratotype Section and Point (GSSP) Huanghuachang, South China. Newsletter on Stratigraphy, Vol. 43/3, 235-250.

Li, J., Servais, T., Yan, K., 2014. The Ordovician acritarch genus *Rhopaliophora*: Biostratigraphy, palaeobiogeography and palaeoecology. Review of Palaeobotany and Palynology, 208, 1-24.

Loeblich, A.R., Tappan, H., 1976. Some news and revisited organic-walled phytoplankton microfossil genera. J. Palaeontol., vol. 52, 301-308.

Melvin, J., 2015. Lithostratigraphy and depositional history of Upper Ordovician and lowermost Silurian sediments recovered from the Qusaiba-1 shallow core hole, Qasim region, central Saudi Arabia. Review of Palaeobotany and Palynology 212, 3-21.

Moczydlowska, M., 1991. Acritarch biostratigraphy of the Lower Cambrian and the Precambrian-Cambrain boundary in southeastern Poland. Fossils and strata, 29, 1-127.

Molyneux, S.G., Mohiuddin, U., Penney, R., Paris, F., 2002. Turnover of acritarches and chitinozoan species, endemism and sequence stratigraphy in the Lower Palaeozoic of Oman, Polen, 14, 132-133.

Molyneux, S.G., Osterloff, P., Penny, R, Spaak, P., 2006. Biostratigraphy of the Lower Paleozoic Haima Supergroup, Oman: its application in sequence stratigraphy and hydrocarbon exploration. GeoArabia 11, 17- 48.

Molyneux, S.G., Delabroye, A., Wicander, R., Servais, T., 2013. Biogeography of early to mid Palaeozoic (Cambrian-Devonian) marine phytoplankton. In Harper, D.A.T. & Servais, T. (eds.), 2013. Early Palaeozoic Biogreography and Palaeogeography. Geological Society, London, Memoirs, 38, 365-397.

Mudie, P.J., 1992. Circum-arctic Quaternary and Neogene marine palynofloras: paleoecology and statistical analysis. In: Head, M.J., Wrenn, J.H. (Eds.)? Neogene and Quaternary Dinoflagellate Cysts and Acritarchs. American Association of Stratigraphic Palynology Foundation, College Station TX, 347-390.

Munnecke, A., Servais, T., 1996. Scanning Electron Microscopy of polished , slightly etched rock surfaces: a method to observe palynomorphs in situ. Palynology, 20, 163-176.

Munnecke, A., Delabroye, A., Servais, T., Vandenbroucke, T.A., Vecoli, M., 2012. Systematic occurrences of malformed (teratological) acritarchs in the run-up of Early Palaeozoic $\delta^{13}C$ isotope excursions. Palaeogeography, Palaeoclimatology, Palaeoecology, 367-368, 137-146.

Murphy, L.S. and Haugen, E.M., 1985. The distribution and abundance of phototrophic ultraplankton in the North Atlantic. Limnol. Oceanogr., 30, 47-58.

Not, F., 2004. Structure et diversité des communautés de picoeucaryotes en milieu marin. Biodiversité et écologie. PhD, Paris VI, 1-160. http://hal.upmc.fr/tel-01111001.

Paris, F., Boumendjel, K., Dabard, M.P., Ghienne, J.F., Loi, A., Videt, B., Achab, A., 2007. Chitinozoan-based calibration of early-mid Ordovician transgressive events on northern Gondwana. Acta Palaeontologica Sinica, 46, 370-375.

Pawley, J.B., 2006. Handbook of biological confocal microscopy. New York; Springer. 2006, 985p.

Playford, G., Martin, F., 1984. Ordovician acritarchs from the Canning Basin, WXestern Australia. Alcheringa, 8, 187-223.

Pohl, A., Donnadieu, G., Le Hir, J.F., Buoncristiani, J.F., Vennin, E., 2016. Effect of the Ordovician paleogeography on the (in)stability of the climate. Clim. Past., 3, 375-386.

Pohl, A., Donnadieu, Y., Le Hir, G., Ladant, J.B., Dumas, C., Alvarez-Solas, J., Vandenbroucke, T.R.A., 2016. Glacial onset predated Late Ordovician climate cooling. Paleoceanography, 31, doi: 10.1002/2016PA002928, 1-22.

Powers, R.W., Ramirez, L.F., Redmond, C.D., Elberg, Jr., E.L., 1966. Geology of the Arabian Peninsula – Sedimentary Geology of Saudi Arabia: US Geological Survey Professional Paper, 560-D, Washington, 147p.

Prauss, M., 2000. The oceanographic and climatic interpretation of marine palynomorph phytoplankton distribution from Mesozoic, Cenozoic and Recent sections. Göttinger Arb. Geol. Paläont., 76, 235 p.

Prebble, J.G., Hannah, M.J., Barrett, P.J., 2006. Changing Oligocene climate recorded by palynomorphs from two glacio-eustatic sedimentary cycles, Cape Roberts Project, Victoria Land Basin, Antarctica. Palaeogeography, Palaeoclimatology, Palaeoecology, 231, 58-70.

Quadros, L.P., 1986a. Ocorrência de microfósseis (Acritarchae) ordovicianos na Sub-bacia do Alto Amazonas, Brasil. *Boletim Técnico da Petrobras*, 29 (3), 181-191.

Quadros, L.P., 1986b. Ocorrência de microfósseis (Acritarchae) ordovicianos na Sub-bacia do Alto Amazonas, Brasil. *In:* 4º Congreso Argentino de Paleontología y Bioestratigrafía. Mendoza, Asociación Paleontológica Argentina / Conicet. Actas, 1, 151-156.

Quadros, L.P., 1988. Zoneamento bioestratigráfico do Paleozóico Inferior e Médio (seção marinha) da Bacia do Solimões. *Boletim de Geociências da Petrobras*, 2 (1), 95-109.

Quintavalle, M., Playford, G., 2006. Palynostratigraphy of Ordovician strata, Canning Basin, Western Australia. Part One: acritarchs and prasinophytes. Palaeontographica, B, 275, 1-88.

Quintavalle, M., Playford, G., 2006. Palynostratigraphy of Ordovician strata, Canning Basin, Western Australia. Part Two: chitinozoans and biostratigraphy. Palaeontographica, B, 275, 89-131.

Raiswell, R., Berner, R.A., 1986. Pyrite and organic matter in Phanerozoic normal marine shales. Geochemica et Cosmochimica Acta, Vol. 50, 1967-1976.

Rasmussen, C.M.Ø, Ullmann, C.V., Jakobsen, K.G., Lindskog,A., Hansen, J., Hansen, T., Eriksson, M.E., Dronov, A., Frei, R., Korte, C., Nielsen, A., Harper, D.A.T., 2016, Onset of main Phanerozoic marine radiation sparked by emerging Mid Ordovician icehouse. Nature, Scientific Reports, 6:18884/DOI:10.1038/srep 18884, 1-9.

Rickards, B.R., Booth G.A., Paris, F., Heward, A.P., 2010. Marine flooding events of the Early and Middle Ordovician of Oman and the United Arab Emirates and their graptolite acritarch and chitinozoan associations. GeoArabia, 15, 4, 81-120.

Riedman, L.A., Porter, S.M., Halverson, G.P., Hurtgen, M.T, Junium, C.K., 2014. Organic-walled microfossil assemblages from glacial and interglacial Neoproterozoic units of Australia and Svalbard, Geology, 7 October 2014, doi: 10.1130/G35901.1

Riegel, W., Wiese, F., Arp, G., Wilde, V., 2014. Microphytoplankton from the Jena Formation (Lower Muschelkalk Subgroup, Anisian) in the forestry quarry at Herberhausen near Göttingen (Germany). In Wiese F., Reich M., Arp G. (eds.): “Spongy, slimy, cosy and more…”. Göttingen Contributions to Geosciences, 77, 63-76.

Roche, M., 1994. Palynologie et palynofacies du Rhétien (Trias supérieur) du nord-est du Bassin de Paris. Ph.D. Thesis. Université de Liège, unpublished, 138 p.

Ross, P.E., Duthie, H.C., 1981. Ultraplankton biomass, productivity and efficiency in lac Matamec, a Precambrian shield lake. Journal of Phycology, 17, 181-186.

Rubinstein, C.V., Vecoli, M,, Astini, R.A., 2011. Biostratigraphy and paleoenvironmental characteriziation of the Middle Ordovician from the Sierras Subandinas (NW Argentina) based on organic-walled microfossils and sequence stratigraphy. Journal of South American Earth Sciences, 31, 124-138.

Schrank, E., 2003. Small acritarchs from the Upper Cretaceous: taxonomy, biological affinities and paleoecology. Review of Palaeobotany and Palynology, 123, 199-235;

Scott, A.C., 1989. Observations on the nature and origin of fusain. Int. J. Coal Geol., 12, 443-475.

Scott, A.C., 2010. Charcoal recognition, taphonomy and uses in palaeoenvironmental analysis. Palaeogeogr. Palaeoclimatol. Palaeoecol., 291, 11-39.

Senalp, M., Al-Duaiji, A.A., 2001. Qasim Formaion: Ordovician Storm-and Tide-Dominated Shallow-Marine Siliciclastic Sequences, Central Saudi Arabia, GeoArabia, 6, 2, 233-268.

Servais, T., 1993. The Ordovician acritarch *Frankea*. In : Molyneux, S.G., Dorning, K.J. (Eds.), Contributions to acritarch and chitinozoan research. Special Papers in Palaeontology, 47, 395-414.

Servais, T. 1997. The Ordovician *Arkonia-Striatotheca* acritarch *plexus*. Review of Palaeobotany and Palynology, 98, 47-79.

Servais, T., 2016. The absence of a late Paleozoic “phytoplankton blackout” and the need of picopalaeontology; MVP-PPMB meeting:Miscellanea paleontological 2016, Ph. Steemans and Ph. Gerienne (eds.), Liège, Belgium, December 21, 2016. Abstract, p. 19.

Servais,T., Molyneux, S.G., 1997. The messaoudensis-trifidum acritarch assemblage (Ordovician: late Tremadoc-early Arenig) from subsurface of Rügen (Baltic Sea, NE Germany) . Palaeontographia italic, 84, 113-121.

Servais, T., Brocke, R. and Fatka, O. 1996. Variability in the Ordovician acritarch *Dicrodiacrodium.* Paleontology, 39, part 2, 389-405.

Servais, T., Martin, R.E., Nützel, A., 2016. The impact of the « terrestrialisation process » in the late Paleozoic PCO_2, PO_2, and the “phytoplankton blackout”. Review of palaeobotnay and Palynology, 224, 26-37.

Sharland, P.R., Archer, R., Casey, D.M., Davies, R.B., Hall, A., Heward, A., Horbury, A., Simmons, M.D., 2001. Arabian Plate Sequence Stratigraphy. GeoArabia Special Publication SP2, Gulf PetroLink, Barhain, 371p.

Sheehan, P.M., 2001. The late Ordovician mass extinction. Annual Review of Earth and Planetary Sciences, 331-364.

Sieburth, J. McN., Smetacek, V., Lenz, J., 1978. Pelagic ecosystem structure: heterotrophic compartments of the plankton and their relationship to plankton size fractions. Limnol. Oceanogr., 23, 1256-1263.

Soufiane, A., Achab, A., 1993. Quelques assemblages de chitinozoaires de l'Ordovicien du Maroc, Bassin de Tadla. *Geobios*, 26 (5), 535-553.

Steemans, P., Wellman, C.H., Gerienne, P., Le Hérissé, A., Vecoli, M., 2017. Middle Ordovician cryptospores from the Saq6Hanadir transitional beds in the Qsim-801 well, Saudi Arabia…..

Steinecke, M., Bramkamp, R.A., Sanders, N.J., 1958. Stratigraphic relations of Arabian Jurassic Oil. In : Weeks, L.G. (Ed.). Habitat of Oil, the American Association of Petroleum Geologist, Tulsa, Oklahoma, USA, 1294-1329.

Strother, P.K., Wellman C. H., 2016. Palaeoecology of a Billion-year-old non marine cyanobacterium from the Torridon Group and Nonesuch Formation. Palaeontology, 59, part 1, 89-108.

Strother, P.K., Servais, T., Vecoli, M. 2010. The effects of terrestrialization on marine ecosystems: the fall of CO_2. In Vecoli, M., Clément, G., Meyer-Berthaud, B. (eds.) The Terrestrialization Process: Modelling Complex Interactions at the Biosphere-GeosphereInterface. Geological Society London, Special Publications, 339, 37-48

Strother, P.K., Al-Hajri, S., Traverse, A., 1996. New evidence for land plants from the lower Middle Ordovician of Saudi Arabia. Geology, 24, 55-58.

Strother, P.K., Traverse, A., and Vecoli, M., 2015. Cryptospores from the Hanadir Shale Member of the Qasim Formation, Ordovician (Darriwilian) of Saudi Arabia: taxonomy and systematics. Review of Palaeobotany and Palynology, 212, 97-110.

Stump, T.E., 1995. Geology and biostraigraphy of the Late precambrian through Paleoezoic sediments of Saudi Arabia. Review of Palaeobotany and Palynology, 89, 5-17.

Tappan, H., 1980.The Paleobiology of Plant Protists. W.H. Freeman, San Fransisco, 1028 p.

Thompson, C.K., 2011. Carbon and sulfur cycling in Early Paleozoic Oceans. PhD thesis, University of Tennessee, 2011. http://trace .tennessee.edu/utk_gradiss/1033.

Tongiorgi, M., Di Milia, A., 1999. Differentiation and spread of the Baltic Acritarch Province (Arenig-Llanvirn). Bolletino della Società Paleontologica Italiana, 38 (2-3), 297-312.

Tyson, R.V., 1993. Palynofacies analysis, in Jenkins, D.G. ed., Applied Micropaleontology: Kluwer Academic Publishers, Dordrecht, 153-193.

Trotter, J.A., Williams, I.S, Barnes, C.R., Lécuyer, C, Nicoll, R.S. 2008. Did cooling oceans trigger Ordovician biodiversification? Evidence from conodont thermometry, Science, 321, 550- 554.

Turner, B.R., Armstrong, H.A., Wilson, C.R., Makhlouf, I.M., 2012. High frequency eustatic sea-level changes during the Middle to early Late Ordovician of southern Jordan: Indirect evidence for a Darriwilian Ice Age in Gondwana. Sedimentary Geology, 251-252, 34-48.

Urbanek, A., 1993. Biotic crisis in the history of the Upper Silurian graptolites. A palaeobiologic model. Historical Biology 7, 29-50.

Vandenbroucke, T.R.A., Armstrong, H.A., Williams, M., Paris, F., Zalasiewicz, J.A., Sabbe, K., Nõlvak, J., Challands, T., Verniers, J, Servais, T., 2010. Polar front shift and atmospheric CO_2 during the glacial masimum of the Early Paleozoic Icehouse. PNAS, August 24, 2010, 107, 34, 14983-14986.

Vandenbroucke, T.R.A., Armstrong, H.A., Williams, M., Paris, F., Sabbe, K., Zalasiewicz, Nõlvak, J., Verniers, J, 2010. Epipelagic chitinozoan biotopes map a steep latitudinal temperature gradient for earliest Late Ordovician seas: Implications for a cooling Late Ordovician climate. Palaeogeography, Palaeoclimatology, Palaeoecology, 294, 202-219.

Vaslet, D., 1990. Le Paléozoïque (Anté-Permien supérieur) d'Arabie Saoudite. Documents du B.R.G.M., 191, 1-230.

Vaslet, D., Berthiaux, A., Le Strat, P., Kellog, K.S., Vincent, P.L., 1987. Geological map of the Baqa quadrangle, sheet 27F, Kingdom of Saudi Arabia. Saudi Arabian D.M.M.R., Geoscience map GM-116A.

Vavdová, M. 1982. Phytoplancton communities of Cambrian and Ordovician age of Central Bohemia. Věstník Ústředniho ústavu geologického, 57, 3, 145-155.

Vecoli, M., 2000. Palaeoenvironmental interpretation of microphytoplankton diversity trends in the Cambrian-Ordovician of the northern Sahara Platform. Palaeogeography, Palaeoclimatology, Palaeoecology, 160, 329-346.

Vecoli, M., Le Hérissé, A., 2004. Biostratigraphy, taxonomic diversity and patterns of morphological evolution of Ordovician acritarchs (organic-walled microphytoplankton) from the northrn Gondwana margin in relation to palaeoclimatic and palaeogeographic changes. Earth-Science reviews, 67, 267-311.

Vecoli, M., Strother, P.K., 2016. Palynology of the Ordovician Kanosh Shale at Fossil Mountain, Utah. J. of Paleontology, doi: 10.1017/ jpa.2015.29, 1-24.

Vecoli, M., Tongiorgi, M., Playford, G., 1999. The Ordovician acritarchs *Frankea breviuscula, F. longiuscula,* and *F. sartbernardensis*: a new study. Bolletino della Società Paleontologica Italiana, 38, 2-3, 343-358.

Vecoli, M., Tongiorgi, M., Abdesselam-Roughi ; F., Benzarti, R., Massa, D., 1999. Palynostratigraphy of Upper Cambrian-upper Ordovician intracratonic clastic sequences, North Africa. Bolletino della Società Paleontologica Italiana, 38, 2-3, 331-341.

Wellman, C.H., Strother, P.K., 2015. The terrestrial biota prior to the origin of land plants (embryophytes): a review of the evidence. Palaeontology, 58, 4, 601-627.

Wellman, C.H., Osterloff, P.L., Mohluddin, U., 2003. Fragments of the earliest plants. Nature, Vol. 425, 18 September 2003, 282-284.

Wood, G.D., Tekbali, A.O., 1987. A unique new genus of Acritarcha (organic-walled microphytoplankton) from the Tanezzuft Formation (Silurian) of Libya. 11, 107-112.

Yin, L.M., Di Milia, A.,Tongiorgi, M., 1998. New and emended acritarch taxa from the lower Dawan Formation (Lower Arenig, Huanghuachang section, South China). Rev. Palaeobot. Palynol., 102, 223-248.

Young, S.A., Saltzman, M.R., Ausich, W.I., Desrochers, A., Kaljo, D. 2010. Did Changes in atmospheric CO_2 coincide with latest Ordovician glacial-interglacial cycles? Palaeogreography, Palaeoclimatology, Paleoeecology 296, 376-388.

Young, S.A., Saltzman, M.R., Foland, K.A., Linder, J.S., Kump, L.R. 2009. A major drop in seawater $^{87}Sr/^{86}Sr$ during the Middle Ordovician (Darriwilian): Links to volcanism and climate? Geology, 37, 10, 951-954.

Appendix A

A.1. List of palynomorph taxa mentioned in the text

All palynomorph genera ans species mentioned in the text and Tabl.1, are alphabetically listed in genera and species, under their respective morphologic categories.

Group Acritarcha Evitt, 1963

Acanthodiacrodium costatum Burmann, 1968

Acanthodiacrodium uniforme Burmann, 1968

Ampullula suetica Righi, 1991

Ankyrotrochos crispum (Vavrdová) Vecoli, 1999

Aremoricanium rigaudae Deunff, 1955

Aremoricanium aff. *A. squarrosum* Loeblich and Mac Adam, 1971

Aremoricanium aff. *A. decoratum* Loeblich and Mac Adam, 1971

Aremoricanium sp. A

Arkonia sp. A in Vecoli (1999)

Aureotesta clathrata (Vavrdová) emend. Brocke et al., 1997

Baltisphaeridium kalbavense (Vavrdová) kjellström, 1971

Baltisphaeridium ternatum (Burmann) emend Rauscher, 1973

Barakella felix Cramer and Diez, 1977

Barakella fortunata Cramer and Diez, 1977

Barakella rara (Lu Li-chang) emend Tongiorgi et al., 1995

Caldariola glabra (Martin) Molyneux in Molyneux and Rushton, 1988

Carminella mapplewoodensis Cramer, 1964

Claviticystis bulbis Habib and Knapp, 1982

Comasphaeridium aff. *C. piluliferum* Playford and Martin, 1984

Comaspaheridium aff. *C. pratulum* Cramer and Diez, 1977

Comasphaeridium sp.

Conaticystis orbis Habib and Knapp, 1982

Cristallinium sp.

Cymatiogalea spp.

Dactylofusa striatogranulata Jardiné, Combaz, Magloire, Peniguel et Vachey, 1974

Dasydorus cirritus Playford and Martin, 1984

Dicrodiacrodium ancoriforme Burmann, 1968 emend. Servais et al., 1996

?Dorsenidium sp.

Eupoikilofuzsa rochesterensis Cramer, 1970

Genus *Focusphaera* Quadros, 1986

Focusphaera elongata Quadros, 1986

Genus *Frankea* (Burmann, 1970) Servais, 1993 emend

Frankea breviuscula Burmann, 1970

Helosphaeridium radzynianum Moczydlowska, 1991

Leiofusa spp.

Lusatia dendroidea Burmann, 1970

Lusatia heteromorpha Vavdrova, 1986

Frankea longiuscula Burmann, 1970

Frankea longiuscula var. *darriwilense* nov. var.

Frankea sartbernardensis (Martin) Colbath, 1986

Glaucotesta latiramosa Vavrdová, 1982

Lophosphaeridium sp.

Genus *Micrhystridium* Deflandre, 1937

Micrhystridium regulum nov. sp.

Micrhystridium spp.

Multiplicisphaeridium irregulare Staplin *et al., 1965*

Multiplicisphaeridium multipugiunculatum Cramer and Diez, 1977

Genus Nan

Orthosphaeridium sp.

Peteinosphaeridium trifurcatum (Eisenack, 1931 ex Eisenack, 1938) Eisenack, 1969

Peteinosphaeridium velatum Kjellström, 1971

Peteinosphaeridium cf. *P.* sp. A in Vecoli (1999)

Peteinosphaeridium sp. B

Pirea sp.

Poikilofusa ciliaris Vecoli, 1999

Poikilofusa spinata Staplin et al., 1965

Polygonium dentatum (Timofeev *ex* Konzalová-Mazancová) Albani, 1989

?Pulvinosphaeridium sp. A

Reticella corrugata Agic, 2015

Rhopaliophora palmata (Combaz and Peniguel) emend Palyford and Martin, 1984

Riculasphaera fissa Loeblich and Tappan, 1969

Stellechinatum celestum (Martin) Turner, 1984

Stelliferidium stelligerum (Górka) emend Deunff et al., 1974

Stelliferidium striatulum (Vavrdová) Deunff et al., 1974

Stelliferidium sp. A

Striatotheca frequens Burmann, 1970

Striatotheca monorugulata Yin et al., 1998

Striatotheca mutua Burmann, 1970

Striatotheca principalis parva Burmann, 1970

Striatotheca quieta (Martin) Rauscher, 1974

Striatotheca rarirrugulata (Cramer, Kanes, Diez and Christopher) Eisenack et al., 1976

Symplassosphaeridium spp.

Synsphaeridium spp.

Tabulimicrocystis tetragonis Habib and Knapp, 1982

Genus *Tyrannus* Wood and Tekbali, 1987

Tyrannus giganteus (Jardiné et al., 1974) Wood and Tkbali, 1987

Tyrannus proteus nov. sp.

Uncinisphaera fusticula Vecoli, 1999

Undeterminate sp. A

Verrucidium globosum Habib and Knapp, 1982

Veryhachium checkleyensis Dorning, 1981

Veryhachium lairdii (Deflandre) Deunff, 1959 ex Downie, 1959

Veryhachium trispinosum group

Vogtlandia ramificata Burmann, 1970

Vogtlandia tenuata Burmann, 1970

Vogtlandia sp. A in Vecoli, 1999

Chlorococcales

Palembages morulosa Wetzel, 1961

Prasinophycean algae

Cymatiosphaera spp.

Cymatiosphaeropsis rotundus Habib and Knapp, 1982

Pterospermopsis colbathii Vavrdová, 1990

Pterospermopsis franciniae Quintavalle and Playford, 2006

Zygnematales

Genus *Gelasinicysta* Head, 1992

Algae and questionable algae

Clusters of sphaeromorphs

Clypeolus sp

Striate sphaeromorphs

Virgatosporites rudii Combaz, 1967

Cyanobacteria

Bavlinella foveolata (Shepeleva, 1962) Vidal, 1976

Sphaerocongregus variabilis Moorman, 1974

Enigmatic forms

Grey elements

Chitinozoa

Belonechitina henryi Paris, 1981

Desmochitina bulla Taugourdeau & Jekhowsky, 1960

Desmochitina ornensis Paris, 1981

Linochitina pissotensis Paris, 1981

Siphonochitina formosa Jenkins, 1967

Possible fungi

Genus *Germinosphaera* (Mikhailova, 1986) emend Butterfield, Knoll and Swett, 1996

Genus *Tappania* Butterfield, 2005

Graptolites

Didymograptus cf. *bifidus* (Hall) Ruedemann, 1947

Didymograptus hirundo Salter, 1863

Didymograptus murchinsoni (Beck, 1839)

Didymograptus protobifidus Elles, 1933

Undulograptus austrodentatus (Harris and Keble, 1932)

Trace fossil

Cruziana sp. D'Orbigny, 1842

Phycodes fusiforme Seilacher, 2000

PLATES

SA: Saudi Aramco collection; LPB: Laboratory of Paleontology of Brest collection; EF: England Finder coordinates

Plate 1

Fig. 1. *Baltisphaeridium klabavense* (Vavrdová) Kjellström, 1971. QSIM-801, 728.5 feet, slide LPB 13071 (EF O33/4). SEM view of a specimen, diameter of the central body 67 µm, process length 45 µm.

Fig. 2. *Barakella rara* (Lu Li-chang) emend Tongiorgi et al., 1995. QSIM-801, 719.9 feet, SA slide 44881 (EF E54/1). Central body 45x35 µm; process length 39 µm.

Fig.3. *Barakella fortunata* Cramer and Diez, 1977. QSIM-801, 719.9 feet, SA slide 44881 (EF P62/3). Central body 45x33 µm; process length 39 µm.

Fig. 4. *Dicrodiacrodium ancoriforme* Burmann, 1968 emend Servais et al., 1996. QSIM-801, 719.9 feet, SA slide 44881 (EF D49). Central body 33x25 µm; process length 17 µm.

Fig. 5. *Cymatiosphaera* sp. QSIM-801, 702.7 feet, slide 44858.2 (EF G58/1). Diameter of the central body 33 µm; height of the membranous crests 6 µm.

Fig. 6. *Veryhachium trispinosum* group. QSIM-801, 719.9 feet, SA slide 44881 (EF F48/4). Central body 31 µm; process length 11 µm.

Fig.7. *Virgatosporites rudi* Combaz, 1967. QSIM-801, 699.9 feet, SA slide 44857.2 (EF P49/4). Total diameter 45 µm.

Fig. 8. *Dasydorus cirritus* Playford and Martin, 1984. QSIM-801, 682.2 feet, SA slide 44850 (EF S53). Vesicle length 50 µm, width 30 µm.

Figs. 9, 10. *Glaucotesta latiramosa* Vavrdová, 1982. 9. SEM view of a specimen, QSIM-801, 712.7 feet, slide LPB 13075 (EF L26/4). Vesicle diameter 22 µm, process length 15 µm; 10. QSIM-801, 712.7 feet, slide LPB 13074 (EF F46/2). Vesicle diameter 22 µm, process length 15 µm.

Fig. 11. *Frankea breviuscula* Burmann 1970. A variant with 5 processes, QSIM-801, 717.9 feet, SA slide 44862.2 (EF F52). Vesicle diameter 28 µm, process length 14 µm.

Figs. 12, 15. *Focusphaera elongata* Quadros, 1986. 12. QSIM-801, 675.1 feet, SA slide 44853.2 (EF K50/3). A specimen with a microgranulate surface. Rounded basal part of 28 µm in diameter, apical part with the opening 12 µm in diameter, total length 56 µm; 15. SEM view of a specimen, QSIM-801, 712.7 feet, slide LPB 13075 (EF L25). Basal part 45 µm in diameter, apical part 22 µm in diameter, total length 89 µm.

Fig. 13. *Aremoricanium* aff. *A. squarrosum* Loeblich and Mac Adam, 1971. QSIM-801, 717.9 feet, SA slide 44862.2 (EF P48/3). Central body 75 µm in diameter, neck 22 µm long, processes 15-17 µm in length.

Fig. 14. *Aremoricanium rigaudae* Deunff, 1955. QSIM-801, 717.9 feet, SA slide 44862.2 (EF H39). Central body 75 x55 µm, neck 30 µm long, processes 33µm in length.

Planche 1

Fig. 1. *Baltisphaeridium klabavense* (Vavrdová) Kjellström, 1971. Sondage QSIM-801, 728.5 pieds, lame LPB 13071 (EF O33/4). Photo MEB d'un spécimen, diamètre du corps central 67 µm, longueur des processus 45 µm.

Fig. 2. *Barakella rara* (Lu Li-chang) emend Tongiorgi et al., 1995. Sondage QSIM-801, 719.9 pieds, SA lame 44881 (EF E54/1). Corps central 45x35 µm; longueur des processes 39 µm.

Fig.3. *Barakella fortunata* Cramer and Diez, 1977. Sondage QSIM-801, 719.9 pieds, SA lame 44881 (EF P62/3). Corps central 45x33 µm; longueur des processus 39 µm.

Fig. 4. *Dicrodiacrodium ancoriforme* Burmann, 1968 emend Servais et al., 1996. Sondage QSIM-801, 719.9 pieds, SA lame 44881 (EF D49). Corps central 33x25 µm; longueur des processus 17 µm.

Fig. 5. *Cymatiosphaera* sp. Sondage QSIM-801, 702.7 pieds, lame 44858.2 (EF G58/1). Diamètre du corps central 33 µm; hauteur des crêtes membraneuses 6 µm.

Fig. 6. *Veryhachium trispinosum* groupe. Sondage QSIM-801, 719.9 pieds, SA lame 44881 (EF F48/4). Corps central 31 µm; longueur des processus11 µm.

Fig.7. *Virgatosporites rudi* Combaz, 1967. Sondage QSIM-801, 699.9 pieds, SA lame 44857.2 (EF P49/4). Diamètre total 45 µm.

Fig. 8. *Dasydorus cirritus* Playford and Martin, 1984. Sondage QSIM-801, 682.2 pieds, SA lame 44850 (EF S53). Longueur de la vésicule 50 µm, largeur 30 µm.

Figs. 9, 10. *Glaucotesta latiramosa* Vavrdová, 1982. 9. Vue au MEB d'un specimen, sondage QSIM-801, 712.7 pieds, lame LPB 13075 (EF L26/4). Diamètre de la vésicule 22 µm, longueur des processus 15 µm; 10. QSIM-801, 712.7 pieds, lame LPB 13074 (EF F46/2). Diamètre de la vésicule 22 µm, Longueur des processus 15 µm.

Fig. 11. *Frankea breviuscula* Burmann 1970. Un variant avec 5 processus, sondage QSIM-801, 717.9 pieds, SA lame 44862.2 (EF F52). Diamètre de la vésicule 28 µm, longueur des processus 14 µm.

Figs. 12, 15. *Focusphaera elongata* Quadros, 1986. 12. Sondage QSIM-801, 675.1 pieds, SA lame 44853.2 (EF K50/3). Un spécimen avec surface microgranuleuse. La partie basale arrondie mesure 28 µm de diamètre, l'ouverture au sommet à un diamètre de 12 µm, et la longueur totale est de 56 µm.; 15. Vue d'un spécimen au MEB of a specimen, sondage QSIM-801, 712.7 pieds, lame LPB 13075 (EF L25). Partie basale 45 µm de diamètre, partie apicale 22 µm de diameter et longueur totale 89 µm.

Fig. 13. *Aremoricanium* aff. *A. squarrosum* Loeblich and Mac Adam, 1971. Sondage QSIM-801, 717.9 pieds, SA lame 44862.2 (EF P48/3). Corps central, 75 µm de diamètre, cou 22 µm de long, processus 15-17 µm de longueur.

Fig. 14. *Aremoricanium rigaudae* Deunff, 1955. Sondage QSIM-801, 717.9 pieds, SA lame 44862.2 (EF H39). Corps central 75 x55 µm, cou 30 µm de long, processus 33µm de longueur.

Plate 2

Fig. 1. *Polikiofusa ciliaris Vecoli*, 1999. QSIM-801, 728.5 feet, slide LPB 13071 (EF M33/4). Central body 38x80 µm, polar extensions 22 µm long.

Fig. 2. *Baltisphaeridium ternatum* (Burmann) emend. Vecoli, 1999. QSIM-801, 728.5 feet, slide LPB 13071 (EF M30/2). Central body 44 µm, process length 123 µm.

Fig. 3. *Unicinispahera fusticula* Vecoli, 1999. QSIM-801, 728.5 feet, slide LPB 13071 (EF L35/2). Central body 45 µm, process length 17-20 µm.

Figs. 4, 5. *Stelliferidium striatulum* (Vavdová) Deunff, Górka & Rauscher, 1974. 4. QSIM-801, 728.5 feet, slide LPB 13071 (EF O34/1). Central body 42 µm, process length 5 µm; 5. QSIM-801, 728.5 feet, slide LPB 13072 (EF L30/4). Central body 39 µm, process length 5,5 µm .

Fig. 6. *Stelliferidium stelligerum* (Górka) emend Deunff, Górka & Rauscher, 1974. QSIM-801, 712.7 feet, slide LPB 13073 (EF L30/2). Central body 50µm, process length 5 µm, pylome 28 µm in diameter

Fig. 7. *Stellechinatum celestum* (Martin) Turner, 1984. QSIM-801, 712.7 feet, slide LPB 13073 (EF N31). Central body 33 µm, process length 28 µm.

Fig. 8, 9. *Peteinosphaeridium velatum* Kjellström, 1971 emend Playford, Ribecai & Tongiorgi, 1995. 8. QSIM-801, 728.5 feet, slide LPB 13072 (EF O34). Central body 70 µm, process length 20 µm ; 9. QSIM-801, 728.5 feet, slide LPB 13072 (EF L32/3). Central body 43 µm, process length 13 µm

Figs. 10, 11. *Peteinosphaeridium* aff. *P. bergrstroemii*, Staplin, Jansonius & Pocock, 1965 emend Playford, Ribecai & Tongiorgi, 1995. 10. QSIM-801, 728.5 feet, slide

LPB 13072 (EF O32). Central body 60 µm, process length 12-15 µm. 11. Same specimen, detail of the process ornamentation.

Figs. 12, 13. *Peteinosphaeridium* sp. A. 13. Complete specimen, QSIM-801, 712.7 feet, slide LPB 13073 (EF O32/2). Central body 45-47 µm, process length 15 µm; 12. Detail of the ornamentation of the processes.

Plate 2

Fig. 1. *Polikiofusa ciliaris Vecoli*, 1999. QSIM-801, 728.5 pieds, lame LPB 13071 (EF M33/4). Corps central 38x80 µm, extensions aux poles 22 µm de long.

Fig. 2. *Baltisphaeridium ternatum* (Burmann) emend. Vecoli, 1999. QSIM-801, 728.5 pieds, lame LPB 13072 (EF M30/2). Corps central 44 µm, longueur des processus 123 µm.

Fig. 3. *Unicinispahera fusticula* Vecoli, 1999. QSIM-801, 728.5 pieds, lame LPB 13071 (EF L35/2). Corps central 45 µm, longueur des processus 17-20 µm.

Figs. 4, 5. *Stelliferidium striatulum* (Vavdová) Deunff, Górka & Rauscher, 1974. 4. QSIM-801, 728.5 pieds, lame LPB 13071 (EF O34/1). Corps central 42 µm, longueur des processus 5 µm; 5. QSIM-801, 728.5 pieds, lame LPB 13072 (EF L30/4). Corps central 39 µm, longueur des processus 5,5 µm .

Fig. 6. *Stelliferidium stelligerum* (Górka) emend Deunff, Górka & Rauscher, 1974. QSIM-801, 712.7 pieds, lame LPB 13073 (EF L30/2). Corps central 50µm, longueur des processus 5 µm, diamètre du pylome 28 µm.

Fig. 7. *Stellechinatum celestum* (Martin) Turner, 1984. QSIM-801, 712.7 pieds, lame LPB 13073 (EF N31). Corps central 33 µm, longueur des processus 28 µm.

Fig. 8, 9. *Peteinosphaeridium velatum* Kjellström, 1971 emend Playford, Ribecai & Tongiorgi, 1995. 8. QSIM-801, 728.5 feet, slide LPB 13072 (EF O34). Central body 70 µm, process length 20 µm; 9. QSIM-801, 728.5 feet, slide LPB 13072 (EF L32/3). Central body 43 µm, process length 13 µm.

Figs. 10, 11. *Peteinosphaeridium* aff. *P. bergrstroemii*, Staplin, Jansonius & Pocock, 1965 emend Playford, Ribecai & Tongiorgi, 1995. 10. QSIM-801, 728.5 pieds, lame LPB 13072 (EF O32). Corps central 60 µm, longueur des processus 12-15 µm. 11. Même specimen, detail de l'ornementation des processus.

Figs. 12, 13. *Peteinosphaeridium* sp. A. 13. Specimen complet, QSIM-801, 712.7 pieds, lame LPB 13073 (EF O32/2). Corps central 45-47 µm, longueur des processus 15 µm; 12. Détail de l'ornementation des processus.

Plate 3

Figs. 1, 2, 3, 4, 7, 9, 11, 12. *Frankea longiuscula* var. *darriwilense* nov. var. 1. QSIM 801 well, 686.6 feet, slide SA 44851 (EF P47/2), central body 55 µm, process length 78 µm, length of the pinnae 6-7 µm, one process with bulbous tip and unique pinnae; 2. QSIM 801 well, 715.6 feet, slide SA 44861.2 (EF P49/3), central body subcircular 56 µm in diameter, process length 90 µm, two processes with 4 and 5 pinnae, the third one is incomplete; 3. QSIM 801 well, 715.6 feet, slide SA 44861.2 (N48), central body 55 µm in diameter, process length 72 µm, on process simple, the others with 3 to 4 distal pinnae; 4. QSIM 801 well, 699.9 feet, slide SA 44857.2

(S59), central body 49 µm in diameter, process length 78 µm, 3 to 4 pinnae to the extremities of the processes; 7. Holotype, QSIM 801 well, 715.6 feet, slide SA 44861.2 (EF S48/1), central body subtriangular 55 µm in diameter, showing epityche ("horse-shoe" opening), process length 78 µm, 4 to 5 pinnae, to the top of the processes; 9. Aberrant form, QSIM 801 well, 746.5 feet, slide SA 44890 (EF G51), central body subtriangular 40 µm in diameter, but dilated up to 86 µm in length at right, the tips of two visible processes are slightly bulbous with a unique pinna; 11. QSIM 801 well,675.1 feet, slide 44853.2 (EF R56/4), central body 55 µm, process length 78 µm, length of the pinnae 6-7 µm, some bifurcated, and one process with bulbous tip and unique pinnae; 12. QSIM 801 well,675.1 feet, slide 44853.2 (EF U51/1), a specimen bipolar with rounded vesicle and only two processes, central body 55x48 µm, process length 78 µm, between 3 to 6 pinnae up to 8 µm in length

Figs. 5, 8. Hilate Sporomorphs 1; Fig. 5. QSIM 801 well, 728.5 feet, slide SA 44883.2 (EF K55/2), total diameter 33 µm, central pylome 18 µm in diameter; 8. QSIM 801 well, 756 feet, slide 44894.2 (EF T58/1), overall diameter 37 µm, central part 10 µm.

Fig. 6. Undetermined sp. A. , QSIM 801 well, 728.5 feet, slide SA 44883.2 (EF J53) , diameter of the vesicle 50 µm, length of processes 8-9 µm

Fig. 10. *Aremoricanium* aff. *A. decoratum* Loeblich and Mc Adam, 1971. QSIM 801 well, 728.5 feet, slide LPB 13076 (EF H33/2), diameter of vesicle 55x48 µm, tubular neck-like extension 20 µm, length of the processes 11-13 µm.

Fig. 13. *Pterospermopsis francinae* Quintavalle and Playford, 2006. QSIM 801 well, 728.5 feet, slide SA 44883.2 (EF J58/2), overall diameter including flange 42x53 µm, diameter of the central body 26µm

Plate 3

Figs. 1, 2, 3, 4, 7, 9, 11, 12. *Frankea longiuscula* var. *darriwilense* nov. var. 1. Sondage QSIM 801 , 686.6 pieds, lame SA 44851 (EF P47/2), corps central 55 µm, longueur des processus 78 µm, longueur des pinnae 6-7 µm, un processus avec l'extrémité bulbeuse ne portant qu'une pinna; 2. Sondage QSIM 801, 715.6 pieds, lame SA 44861.2 (EF P49/3), corps central subcirculaire 56 µm de diamètre, longueur des processus 90 µm, duex processus avec 4 et 5 pinnae, the troisième est incomplet; 3. Sondage QSIM 801, 715.6 pieds, lame SA 44861.2 (N48), corps central 55 µm de diamètre, longueur des processus 72 µm, un processus extrèmité simple pointue, les autres avec 3 ou 4 pinnae; 4. Sondage QSIM 801, 699.9 pieds, lame SA 44857.2 (S59), corps central 49 µm de diamètre, longueur des processus 78 µm, 3 à 4 pinnae aux extrémités; 7. Holotype, Sondage QSIM 801, 715.6 pieds, lame SA 44861.2 (EF S48/1), corps central sub-triangulaire 55 µm en diamètre, montrant l'epityche (ouverture en "fer à cheval"), longueur des processus 78 µm, 4 à 5 pinnae à l'extrémité des processus; 9. Forme aberrante, Sondage QSIM 801, 746.5 pieds, lame SA 44890 (EF G51), coprs central sub-triangulaire de 40 µm de diamètre, mais dilate dans un sens jusqu'à 86 µm de longueur ; les extrémités visibles des processus sont légèrement bulbeuses avec une pinna unique; 11. Sondage QSIM 801 ,675.1 pieds, lame 44853.2 (EF R56/4), corps central 55 µm, longueur des processus 78 µm, longueur des pinnae 6-7 µm, certaines bifurquées, et un processus avec extrémité bulbeuse et une seule pinna ; 12. Sondage QSIM 801, 675.1 pieds, lame 44853.2 (EF U51/1), un specimen bipolaire avec une vésicule arrondie et seulement 2 processus, Corps central 55x48 µm, longueur des processus 78 µm, portant entre 3 et 6 pinnae jusqu'à 8 µm de long.

Figs. 5, 8. Sporomorphes hilates. 5. Sondage QSIM 801, 728.5 pieds, lame SA 44883.2 (EF K55/2), diamètre total 33 µm, pylome central 18 µm en diamètre; 8. Sondage QSIM 801, 756 pieds, lame 44894.2 (EF T58/1), diamètre total 37 µm, partie centrale 10 µm.

Fig. 6. Undéterminé sp. A. , sondage QSIM 801, 728.5 pieds, lame SA 44883.2 (EF J53) , diamètre de la vésicule 50 µm, longueur des processus 8-9 µm

Fig. 10. *Aremoricanium* aff. *A. decoratum* Loeblich and Mc Adam, 1971. Sondage QSIM 801 well, 728.5 pieds, LPB 13076 (EF H33/2), diamètre de la vésicule 55x48 µm, extension tubulaire 20 µm, longueur des processus 11-13 µm.

Fig. 13. *Pterospermopsis francinae* Quintavalle and Playford, 2006. Sondage QSIM 801, 728.5 pieds, lame SA 44883.2 (EF J58/2), diamètre total incluant l'anneau externe 42x53 µm, diamètre du corps central 26µm

Plate 4

Figs 1-5. Grey elements. 1. Type 1, QSIM 801 well, 699.9 feet, slide 44857.2 (EF W56/2), diameter of the central body 60 µm, Length of the thin tubular extension to the poles 39 to 78 µm; 2. Type 2 a detached halve seen by the interior with radial striae in the polar zone, QSIM 801 well, 741.5 feet, slide 44888 (EF J51/3), total diameter 69 µm; 3. A detached halve , conical with a rounded structure in the apical zone, QSIM 801 well, 741.5 feet, slide 44888 (EF V44/2), total diameter 78 µm, 35 µm of height, diameter of the polar structure 15 µm; 4. Type 2, a complete specimens with the two halves attached, showing a shirt membranous extension to the pole, QSIM 801 well, 741.5 feet, slide 44888 (EF G41/4), total length 90 µm; 5. Type 2, a detached halve, showing an ornamentation of concentric granular ridges towards the equatorial zone, , QSIM 801 well, 719.9 feet, slide 44881.2 (EF Q58/1), total diameter 75 µm.

Fig. 6. *Arkonia* sp. A Vecoli, 1999. QSIM 801 well, 756 feet, slide 44894.2 (EF R54/3), diameter of vesicle 35 µm, Length of processes 30 µm.

Fig. 7. *Aureotesta clathrata* (Vavrdovà) emend Brocke et al., 1997. QSIM 801 well, 754.8 feet, slide LPB 13077 (EF C36/1), diameter of vesicle 33 µm, Length of processes 13,5 µm.

Fig. 8. *Ampullula suetica* Righi, 1991. QSIM 801 well, 756 feet, slide 44894.2 (EF R47/4), diameter of vesicle 61-100 µm, Length of tubular expension 8 µm (incomplete), pylome (indicated by arrow) diameter 18 µm.

Fig. 9. *Ankyrotrochos crispum* (Vavrdovà) Vecoli, 1999. QSIM 801 well, 756 feet, slide SA 44894.2 (EF N42/1) , diameter of vesicle 45 µm, Length of processes 30-35 µm

Fig. 10. *Comasphaeridium* aff. *C. pratulum* Cramer and Diez, 1974;. QSIM 801 well, 754.8 feet, slide LPB 13077 (EF C36/1), diameter of vesicle 33 µm, Length of processes 13,5 µm.

Fig. 11. *Striatotheca rarirrugulata* (Cramer, Kanes, Diez and Christopher) Eisenack, Cramer and Diez, 1976. QSIM 801 well, 682.2 feet, slide 44850 (EF W51.4) , diameter of vesicle 24.5 µm, Length of processes 22 µm

Fig. 12. *Striatotheca monorugulata* Yin et al., 1998. QSIM 801 well, 756 feet, SA 44894.2 (EF H49/3 , diameter of vesicle 22x26 µm, Length of processes 33 µm

Plate 4

Figs 1-5. Grey elements. 1. Type 1, QSIM 801 well, 699.9 feet, slide 44857.2 (EF W56/2), diameter of the central body 60 µm, Length of the thin tubular extension to the poles 39 to 78 µm; 2. Type 2 a detached halve seen by the interior with radial striae in the polar zone, QSIM 801 well, 741.5 feet, slide 44888 (EF J51/3), total diameter 69 µm; 3. A detached halve , conical with a rounded structure in the apical zone, QSIM 801 well, 741.5 feet, slide 44888 (EF V44/2), total diameter 78 µm, 35 µm of height, diameter of the polar structure 15 µm; 4. Type 2, a complete specimens with the two halves attached, showing a shirt membranous extension to the pole, QSIM 801 well, 741.5 feet, slide 44888 (EF G41/4), total length 90 µm; 5. Type 2, a detached halve, showing an ornamentation of concentric granular ridges towards the equatorial zone, , QSIM 801 well, 719.9 feet, slide 44881.2 (EF Q58/1), total diameter 75 µm.

Fig. 6. *Arkonia* sp. A Vecoli, 1999. QSIM 801 well, 756 feet, slide 44894.2 (EF R54/3), diameter of vesicle 35 µm, Length of processes 30 µm.

Fig. 7. *Aureotesta clathrata* (Vavrdovà) emend Brocke et al., 1997. QSIM 801 well, 754.8 feet, slide LPB 13077 (EF C36/1), diameter of vesicle 33 µm, Length of processes 13,5 µm.

Fig. 8. *Ampullula suetica* Righi, 1991. QSIM 801 well, 756 feet, slide 44894.2 (EF R47/4), diameter of vesicle 61-100 µm, Length of tubular expension 8 µm (incomplete), pylome (indicated by arrow) diameter 18 µm.

Fig. 9. *Ankyrotrochos crispum* (Vavrdovà) Vecoli, 1999. QSIM 801 well, 756 feet, slide SA 44894.2 (EF N42/1) , diameter of vesicle 45 µm, Length of processes 30-35 µm

Fig. 10. *Comasphaeridium* aff. *C. pratulum* Cramer and Diez, 1974;. QSIM 801 well, 754.8 feet, slide LPB 13077 (EF C36/1), diameter of vesicle 33 µm, Length of processes 13,5 µm.

Fig. 11. *Striatotheca rarirrugulata* (Cramer, Kanes, Diez and Christopher) Eisenack, Cramer and Diez, 1976. QSIM 801 well, 682.2 feet, slide 44850 (EF W51.4) , diameter of vesicle 24.5 µm, Length of processes 22 µm

Fig. 12. *Striatotheca monorugulata* Yin et al., 1998. QSIM 801 well, 756 feet, slide SA 44894.2 (EF H49/3 , diameter of vesicle 22x26 µm, Length of processes 33 µm

Plate 5

Figs. 1-13. *Tyrannus proteus* nov sp. 1-2. QSIM-801 well, 693.7 ft., slide LPB 13078 (J31/1); 1. Complete specimen, polygonal, central body 134 µm, process length 67 µm. 2, detail of top of the processes, with more fine membrane; 3, 6. QSIM-801 well, 693.7 ft., polygonal form, slide LPB 13078 (M30/2), central body 106 µm, process length 40 µm, detail of a process open-ended. 4, 7. QSIM-801 well, 693.7 ft., polygonal form, slide LPB 13078 (L32/1), central body 89 µm, process length 33 µm, detail of a process top with thin crenulate membrane; 5. CLSM specimen, by reflexion, QSIM-801 well, 693.7 ft., slide LPB 13079 (S31), central body 45 µm; processes length 45µm; 8. Quadrangular form, QSIM-801 well, 693.7 ft., slide LPB 13078 (J32/3), central body 106 µm, process length 22 µm; 9. Triangular form, QSIM-801 well, 693.7 ft., slide LPB 13078 (M31), central body 95 µm, process length 50 µm. 10. Triangular form, QSIM-801 well, 693.1 ft., slide SA 44853.2 (R49/1), central body 60 µm, process length 30 µm; 11. Holotype, polygonal form, QSIM-801 well, 693.1 ft., slide SA 44853.2 (U47/2), central body 100 µm, process length 45-60 µm. 12. Incomplete polygonal specimen with one process bifurcated, QSIM-801 well, 741.5 ft., slide SA 44888.2 (N46/1), central body 80 µm, process length 45 µm. 13. Material of comparison, polygonal specimen, cutting sample Turabah-1 well, 6352-6386 ft., SA slide 8219 (T50/4), Central body 112 µm, process length 45 µm.

Planche 5

Figs. 1-13. *Tyrannus proteus* nov sp. 1-2. Sondage QSIM-801, 693.7 pieds, lame LPB 13078 (J31/1); 1. Forme polygonale, corps central 134 µm, longueur des processus 67 µm. 2, détail du sommet des processus avec une membrane qui s'affine. 3, 6. Forme polygonale, sondage QSIM-801, 693.7 pieds., lame LPB 13078

(M30/2), corps central 106 µm, longueur des processus 40 µm, détail d'un processus ouvert à l'extrémité. 4, 7. Forme polygonale, QSIM-801 well, 693.7 ft., lame LPB 13078 (L32/1), corps central 89 µm, longueur des processus 33 µm, détail d'un processusof avec une membrane fine et crénulée au sommet; 5. Spécimen observe au microscope confocal, photo par réflexion, sondage QSIM-801, 693.7 pieds, lame LPB 13079 (S31), corps central 45 µm; longueur des processus 45µm; 8. Forme quadrangulaire, sondage QSIM-801, 693.7 pids, lame LPB 13078 (J32/3), corps central 106 µm, longueur des processus 22 µm; 9. Forme triangulaire, sondage QSIM-801, 693.7 pieds, lame LPB 13078 (M31), corps central 95 µm, longueur des processus 50 µm. 10. Forme triangulaire, sondage QSIM-801, 693.1 pieds, lame SA 44853.2 (R49/1), corps central 60 µm, longueur des processus 30 µm; 11. Holotype de forme polygonale, sondage QSIM-801, 693.1 pieds, lame SA 44853.2 (U47/2), corps central 100 µm, longueur des processus 45-60 µm. 12. Specimen incomplete, polygonal, avec un processus bifurqué, sondage QSIM-801, 741.5 pieds, lame SA 44888.2 (N46/1), corps central 80 µm, longueur des processus 45 µm. 13. Matériel de comparaison de forme polygonale, échantillon de cutting sondage Turabah-1, 6352-6386 pieds, SA lame 8219 (T50/4), corps central 112 µm, longueur des processus 45 µm.

Plate 6

Figs. 1-4. *Stelliferidium striatulum* (Vavrdova, 1966) Deunff et al., 1974. Core 5, 728.5 ft.1, 3. Fluorescent spectral measurements and profiles of two specimens of *Stelliferidium striatulum.* Profiles in green illustrate excitation spectrum of the thin processes. Red regions and profiles are the emission spectra characteristic of the vesicle wall. The form of the profiles of the two specimens and the fluorescence intensity show a good stability. 2. *Stelliferidium striatulum*, , LPB 13085 (H35), vesicle diameter 45 µm, process length 15 µm; 4. *Stelliferidium striatulum*, LPB13085 (P31/3), vesicle diameter 36 µm, process length 15 µm.

Figs. 5, 6. *Frankea longiuscula* var *darriwilense* nov. var. 5. The images of fluorescence of this variety captured by CLSM, also detected the variation in the thickness of the wall of the vesicle and base of the processes a and the rest of the process trunk. Profile in green illustrate excitation spectrum of the vesicle with globally the same intensity of the emission spectra of *Stelliferidium striatulum*. Profile in blue is the emission spectra of the processes, very closed to the green excitation spectra of *Stelliferidium striatulum*, e. g. Fig. 1; 6. LPB 13085 (043), vesicle diameter 50 µm, processes length incomplete.

Figs. 7,8. *Tyrannus proteus* nov. sp. 7. Fluorescence spectra collected for this species. The profile in yellow, which is emission spectrum for the vesicle is very displaced at right compared to the *Stelliferidium striatulum* or *Frankea longiuscula* var. *darriwilense.* The spectrum in blue , which concern the processes for a part, contrast also largely with emission spectra of the *Stelliferidium* and *F. longiuscula* var *darriwilense*; 8. LPB 13085 (S31), vesicle diameter 45 µm, process length 45 µm.

Planche 6

Figs. 1-4. *Stelliferidium striatulum* (Vavrdova, 1966) Deunff et al., 1974. QSIM-801 well, Carotte 5, 728.5 pieds, Lame LPB 13085. 1, 3. Mesures du spectre de fluorescence et profil de deux specimens de *Stelliferidium striatulum*. Les profils en vert illustrent les spectres d'excitation des processus fins. Les profils et régions en rouge sont les spectres d'émission caractéristiques de la paroi de la vésicule. La forme des profils et l'intensité de fluorescence montrent une bonne stabilité pour les deux spécimens ; 2 . *Stelliferidium striatulum*, LPB 13085 (H35), diamètre de la vésicule 45 µm, longueur des processus 15 µm ; 4. *Stelliferidium striatulum*, LPB 13085 (P31/3), diamètre de la vésicule 36 µm, longueur des processus 15 µm.

Figs. 5, 6. *Frankea longiuscula* var *darriwilense* nov. var. 5. Les images de fluorescence de cette variété capturées par microscopie confocale, détectent aussi les variations d'épaisseur entre la vésicule, la base des processus et le reste des processus. Le profil en vert, qui concerne la vésicule, montre un spectre d'émission de fluorescence assez semblable à celui des *Stelliferidium striatulum.* Le profil en bleu, spectre d'émission des processus est aussi comparable en intensité avec le spectre d'émission des processus de *Stelliferidium striatulum*, notamment pour le spécimen Fig. 1 ; 6. LPB 13085 (043), diamètre de la vésicule 50 µm, les processus sont incomplets.

Figs. 7,8. *Tyrannus proteus* nov. sp. 7. Spectres de fluorescence collectés pour cette espèce. Le profil en jaune qui est le spectre d'émission pour la vésicule est très déplacé sur la droite, si on le compare aux spectres d'émission de *Stelliferidium sriatulum* ou *Frankea longiuscula* var *darriwilense*. De même, le spectre en bleu qui concerne pour partie les processus est très différent des spectres d'émission des *Stelliferidium* et de *Frankea longiuscula* var. *darriwilense* ; 8. LPB 13085 (S31), diamètre de la vésicule 45 µm, longueur des processus 45 µm.

Plate 7

Fig. 1. Cluster Type 2. QSIM-801 well, 677.9 ft., slide SA 44845 (H56/3). Planar coenobium with cells (78 elements) of 10 to 12µm in diameter

Fig. 2-6. *Micrhystridium regulum* nov. sp. ; 2. on a large *Goniosphaeridium* sp., QSIM-801 well, 756 ft., slide SA 44894.2 (Q54/3); *M. regulum* central body 4.5 µm, process length 3.3 µm; *Goniosphaeridium* sp. , Central body 53 µm, process length 13.5-28 µm; 3. *Micrhystridium regulum* nov. sp., Holotype, QSIM-801 well, 749.9 ft., SA 44891.2 (E61), Central body 4 µm, process length 4.5 µm; 4. SEM view of another specimen, QSIM-801 well, 712.7 ft., slide LPB 13081 (030/1), central body 4 µm, process length 5 µm; 5. QSIM-801 well, 682.2 ft., slide LPB 13083 (G41), central body 2.5 µm, process length 3-3.5 µm; 6. QSIM-801 well, 751.8 ft., slide LPB 13084 (D43/1), central body 4µm, process length 1.5-2 µm

Fig. 7. *Micrhystridium* sp.1, QSIM-801 well, 712.7 ft., slide LPB 13081 (G33/3), central body 4.8 µm, process length 2 µm.

Fig. 8. *Leiosphaeridia* sp., QSIM-801 well, 756 ft., slide SA 44894.2 (F48/3), total diameter 7 µm.

Figs. 9, 10. *Micrhystridium* sp.2 9. CLSM view with autofluorescent signal; 10. Same specimen by reflexion, QSIM 801-well, 712.7 ft., central body 5 µm, process length 1-1.5 µm

Fig. 11. *Leiosphaeridia* sp., QSIM-801 well, 712.7 ft., slide LPB 13082 (L31/3), total diameter 6 µm.

Fig. 12. *Micrhystridium* sp. 3. QSIM-801 well, 712.7 ft., slide LPB 13082 (N30/3), central body 3 µm, process length 0.8-1 µm.

Fig. 13. *Cymatiosphaera* sp. QSIM-801 well, 712.7 ft., slide LPB 13082 (N30/3), central body 6 µm, membranous crest 3 µm.

Fig. 14. Aggregates of stained nannospheres, 200 to 500 nm, associated with decaying organic matter mats. QSIM-801, 751.8 ft., slide LPB 13079 (K33)

Figs. 15, 16. Nannobacteria on Nucleopore Polycarbonate filters (0, 8 µm), respectively 0.6 and 0.5 µm. QSIM -801 well, 712.7 ft., LPB 13080.

Fig. 17. SEM view of a cluster of densely packed small sphaeromorphs, mostly smooth surface. QSIM 801-well, 712.7 ft., slide LPB 13082 (N32/2), units of 6 to 10 µm in diameter

Fig. 18. Cluster of densely packed sphaeromorphs, adherent mostly smooth surface, suggesting permanent tetrads . QSIM 801-well, 690.3 ft., slide SA 44852.2 (G54/4), mean diameter of individual units 10 µm.

Fig. 19. Cluster Type 1, QSIM-801 well, 684 ft , slide SA 44881.2 (EF F44),:loosely packed units non adherent, with a pseudoreticulate ornamentation. Cells 18-20 µm in diameter. Some cells show a pylome.

Fig. 20. SEM view of a cluster Type 2, with densely packed cells, adherent. QSIM-801well, 712.7 ft, slide LPB 13073 (Q31), cell diameter 4.5-9 µm.

Planche 7

Fig. 1. Cluster Type 2. Sondage QSIM-801 , 677.9 pieds, lame SA 44845 (H56/3). Coenobium dans un plan avec des cellules (78 éléments) de 10 à 12µm de diamètre.

Fig. 2-6. *Micrhystridium regulum* nov. sp. ; 2. Sur un *Goniosphaeridium* sp., sondage QSIM-801, 756 pieds, lame SA 44894.2 (Q54/3), un specimen de *M. regulum* corps central 4.5 µm, longueur des processus 3.3 µm; *Goniosphaeridium* sp. , corps central 53 µm, longueur des processus 13.5-28 µm; 3. *Micrhystridium regulum* nov. sp., Holotype, sondage QSIM-801, 749.9 pieds, lame SA 44891.2 (E61), corps central 4 µm, longueur des processus 4.5 µm; 4. Vue au MEB d'un autre spécimen, sondage QSIM-801, 712.7 ft., lame LPB 13081 (030/1), corps central 4 µm, longueur des processus 5 µm; 5. Sondage QSIM-801, 682.2 pieds, lame LPB 13083 (G41), corps central 2.5 µm, longueur des processus 3-3.5 µm; 6. Sondage QSIM-801, 751.8 pieds, lame LPB 13084 (D43/1), corps central 4µm, longueur des processus 1.5-2 µm

Fig. 7. *Micrhystridium* sp.1, sondage QSIM-801, 712.7 pieds, lame LPB 13081 (G33/3), corps central 4.8 µm, longueur des processus 2 µm.

Fig. 8. *Leiosphaeridia* sp., sondage QSIM-801, 756 pieds, lame SA 44894.2 (F48/3), diamètre total 7 µm.

Figs. 9, 10. *Micrhystridium* sp.2. 9. Vue au microscope confocal, avec le signal d' autofluorescence ; 10. Même specimen par réflexion, sondage QSIM 801, 712.7 pieds, corps central 5 µm, longueur des processus 1-1.5 µm

Fig. 11. *Leiosphaeridia* sp., sondage QSIM-801, 712.7 pieds, lame LPB 13082 (L31/3), diamètre total 6 µm.

Fig. 12. *Micrhystridium* sp. 3. Sondage QSIM-801, 712.7 pieds, lame LPB 13082 (N30/3), corps central 3 µm, longueur des processus 0.8-1 µm.

Fig. 13. *Cymatiosphaera* sp. Sondage QSIM-801, 712.7 pieds, lame LPB 13082 (N30/3), corps central 6 µm, crêtes membraneuses 3 µm de hauteur

Fig. 14. Aggrégats de nannosphères très colorées, 200 to 500 nm de diamètre, associés à des mats de matière organique dégradée. Sondage QSIM-801, 751.8 pieds, lame LPB 13079 (K33)

Figs. 15, 16. Nannobactéries sur des filtres Nucleopore Polycarboates on Nucleopore Polycarbonate filters (maille 0, 8 µm), qui mesure respectivement 0.6 et 0.5 µm. Sondage QSIM -801, 712.7 pieds, lame LPB 13080.

Fig. 17. Vue au MEB d'un cluster de petits sphaeromorphes de Type 2, plutôt à surface lisse. Sondage QSIM 801, 712.7 pieds, lame LPB 13082 (N32/2), unités de 10 µm de diamètre

Fig. 18. Cluster de sphaeromorphes de Type 2, à éléments très soudés et adhérents à surface lisse, qui suggèrent des tétrades permanentes. Sondage QSIM 801, 690.3 pieds, lame SA 44852.2 (G54/4), diamètre moyen d'une unite individuelle 10 µm.

Fig. 19. Cluster de Type 1, sondage QSIM-801, 684 pieds, lame SA 44881.2 (EF F44) ; unités assez détachées, non-adhérentes, avec une ornementation pseudo-reticulée. Les cellules mesurent entre 18 et 20 µm. Certaines cellules montrent un pylome.

Fig. 20. Vue au MEB d'un autre cluster de Type 2, avec des cellules soudées. Sondage QSIM-801, 712.7 pieds, lame LPB 13073 (Q31), diamètre des cellules entre 4.5 et 9 µm.

Figure captions

Fig. 1. Geological map showing the location of the QSM-801 water well, central Saudi Arabia

Fig. 1. Carte géologique montrant la localisation du sondage d'eau QSIM-801, dans la partie centrale d'Arabie Saoudite.

Table. 1. Stratigraphic range of acritarchs, prasinophycean phycomata and enigmatic forms in the Saq/Hanadir transitional beds, QSM-801 water well, cores 8 to 1.

Tableau 1. Distribution stratigraphique des acritarches, stades phycoma de prasinophycées et forme énigmatiques, dans les niveaux de transition des formations Saq/Hanadir, dans le sondage QSIM-801, carottes 8 à 1.

Fig. 2. Size distribution of palynomophs in the samples to 751.8 ft. and 712.7 ft in QSIM 801-well

Fig. 2. Distribution de la taille des palynomorphes dans les échantillons à 751.8 ft et 712.7 Ft. Dans le sondage QSIM-801.

Fig. 3. Pie charts of size distribution of the palynomrophs in samples to 751.8ft and 712.7 ft in QSIM-801 well.

Fig.3. Présentation de la distribution en taille des palynomorphes dans des graphiques en secteurs pour les échantillons à 751.6 ft. Et 712.7 ft dans le sondage QSIM-801

Tabl. 2. Database of relative abundances in % of the palynomoprhs to specific or generic level, or groups of palynomorphs, and evolution of the amorphous organic latter content between 767.8 and 675.1 ft in the QSIM-801 well.

Tableau 2. Base de données en pourcentages des palynomorphs au niveau spécifique ou générique et des groupes de palynomorphes, et de l'évolution du contenu en matière organique amorphe dans le sondage QSIM-801 entre 767.8 et 675.1 pieds.

Tabl. 3. Quantitative stratigraphical distribution in relative abundances of palynomorphs and amorphic organic matter between 767.8 and 675.1 ft. in the QSIM-801 borehole. The numbers in the cells are percentages.

Tableau 3. Distribution quantitative stratigraphique en pourcentages des palynomorphes et de la matière organique entre 767.8 et 675.1 pieds dans le sondage QSIM-801.

Tabl. 4. Evaluation of the relative abundance of the main groups of acritarchs and the cryptospores for comparison.

Tableau 4. Evaluation de l'abondance relative des principaux groupes d'acritarches et des cryptospores pour comparaison

Fig. 4. This figure documents examples of variations in *Frankea longiuscula* var. *darriwilense* morphology, usually characterized by triangular vesicle and well-developed three processes, but extremely polymorph (1, 2, 3, 6) in the top of the processes (form and number of pinnae). Some forms can be aberrant (4, 5), bipolar with only two processes and rounded vesicle shape, or in a extreme scenario the vesicle is bald without developed processes. Some specimens can have additional processes (Fig. 7).

Fig. 4 Cette figure documente des exemples de variations de la morphologie de *Frankea longiuscula* var. darriwilense, normalement caractérisé par une vésicule triangulaire portant trois processus bien développés, mais extrêmement polymorphe (1, 2, 3, 6), notamment concernant l'extrémité des processus (forme et nombre des pinnae). Des formes peuvent être aberrantes (4, 5), bipolaires avec seulement 2 processus et une vésicule arrondie, ou scénario extrême, sans processus développés. Des spécimens portent des processus additionnels (Fig. 7).

Fig. 5. Data on δ13C and δ15N development to the Saq/Hanadir transition in the QSIM-801 well.

Figure 6. Données sur le développemnt du δ13C et δ15N à la transition Saq/Hanadir dans le sondage QSIM-801

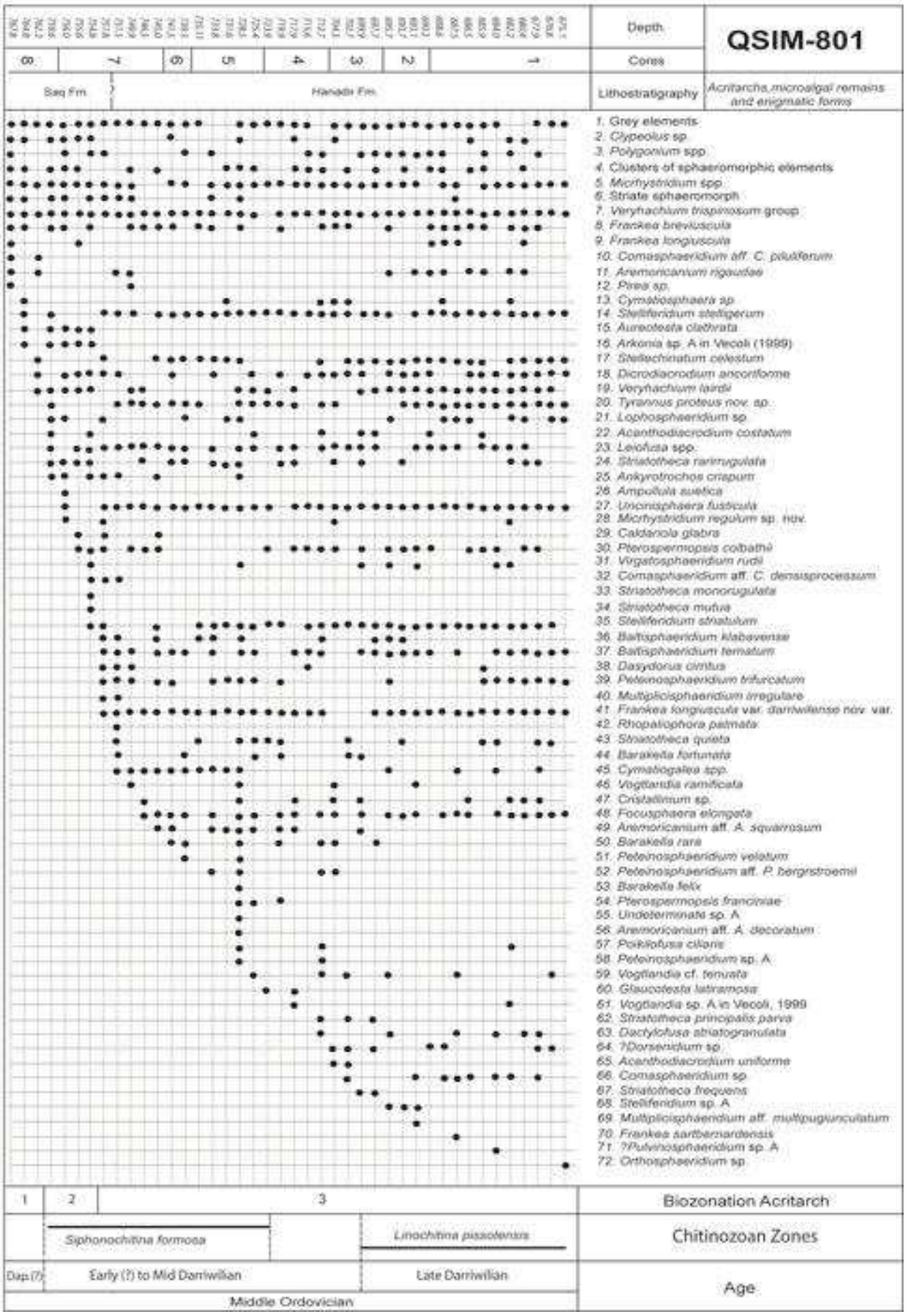

Tabl. 1 Range chart

Plate. 1

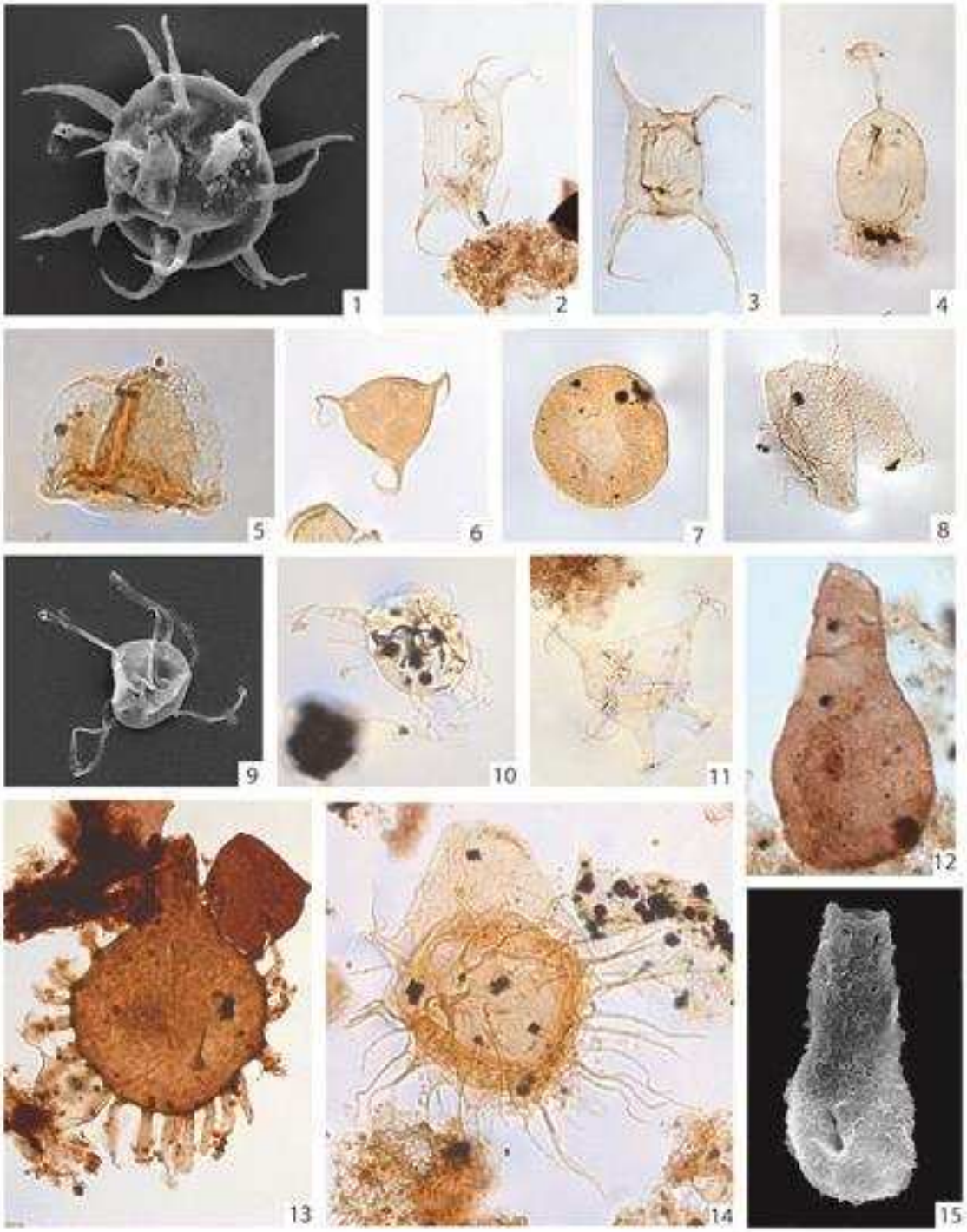

Plate 2

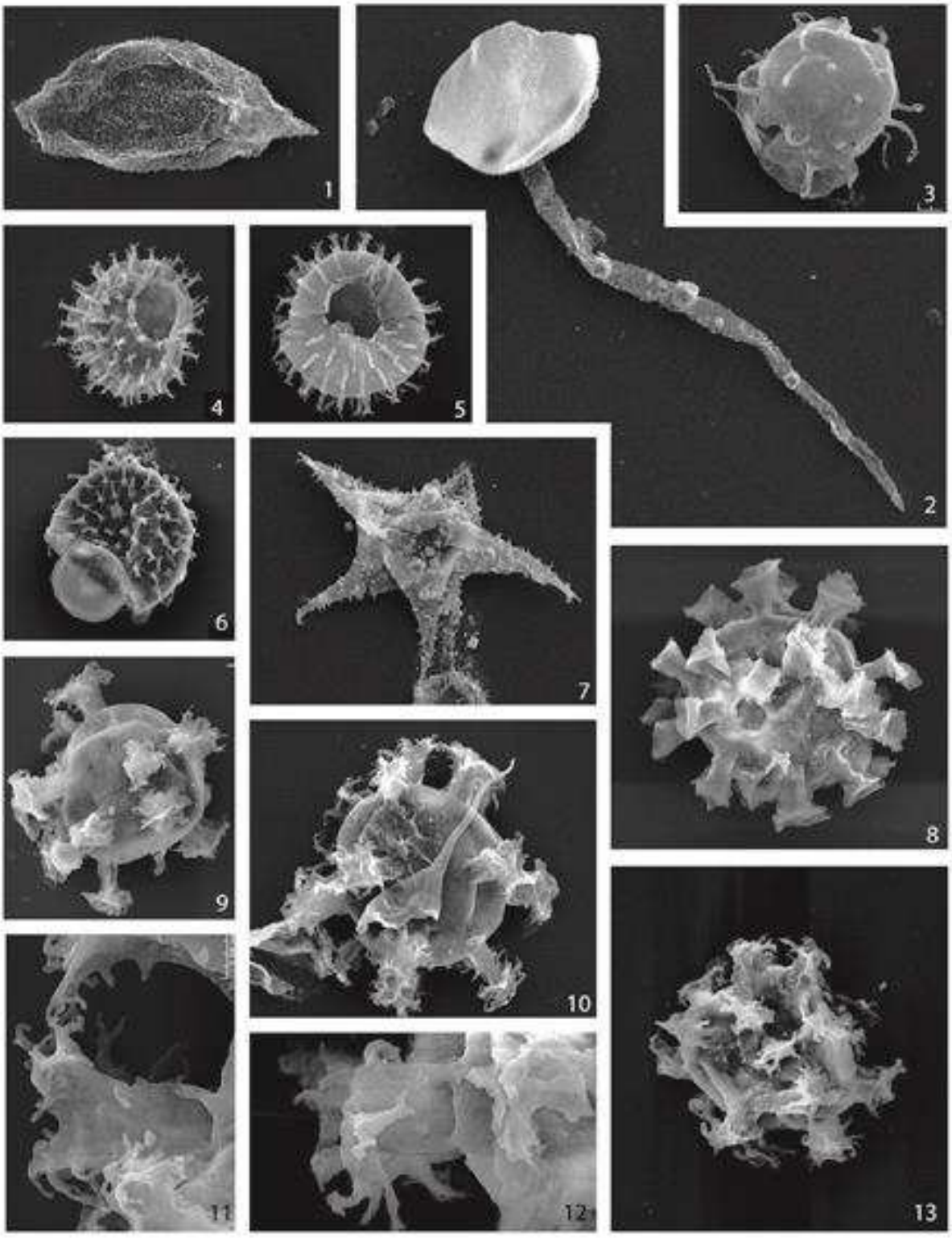

Plate 3

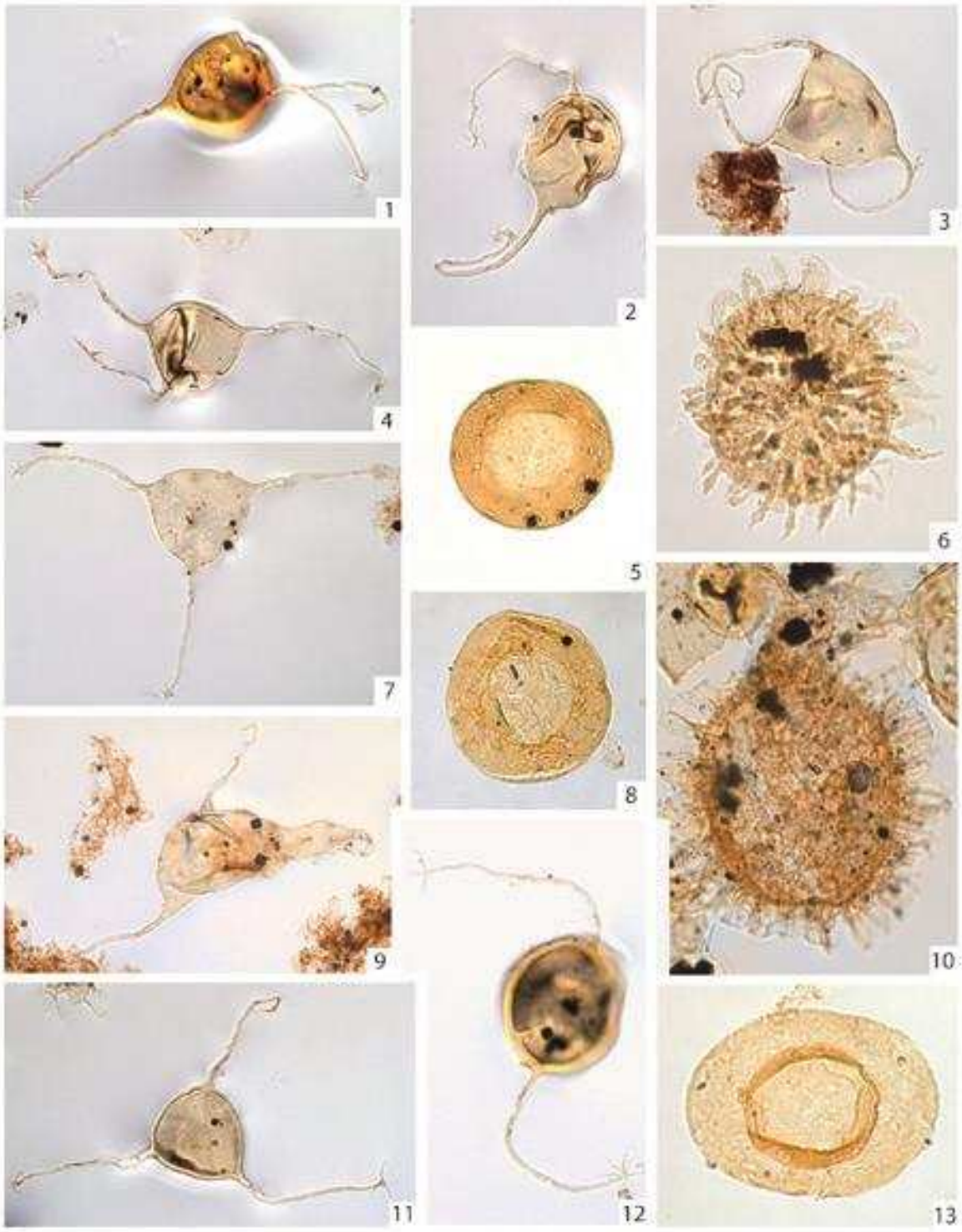

Plate 4

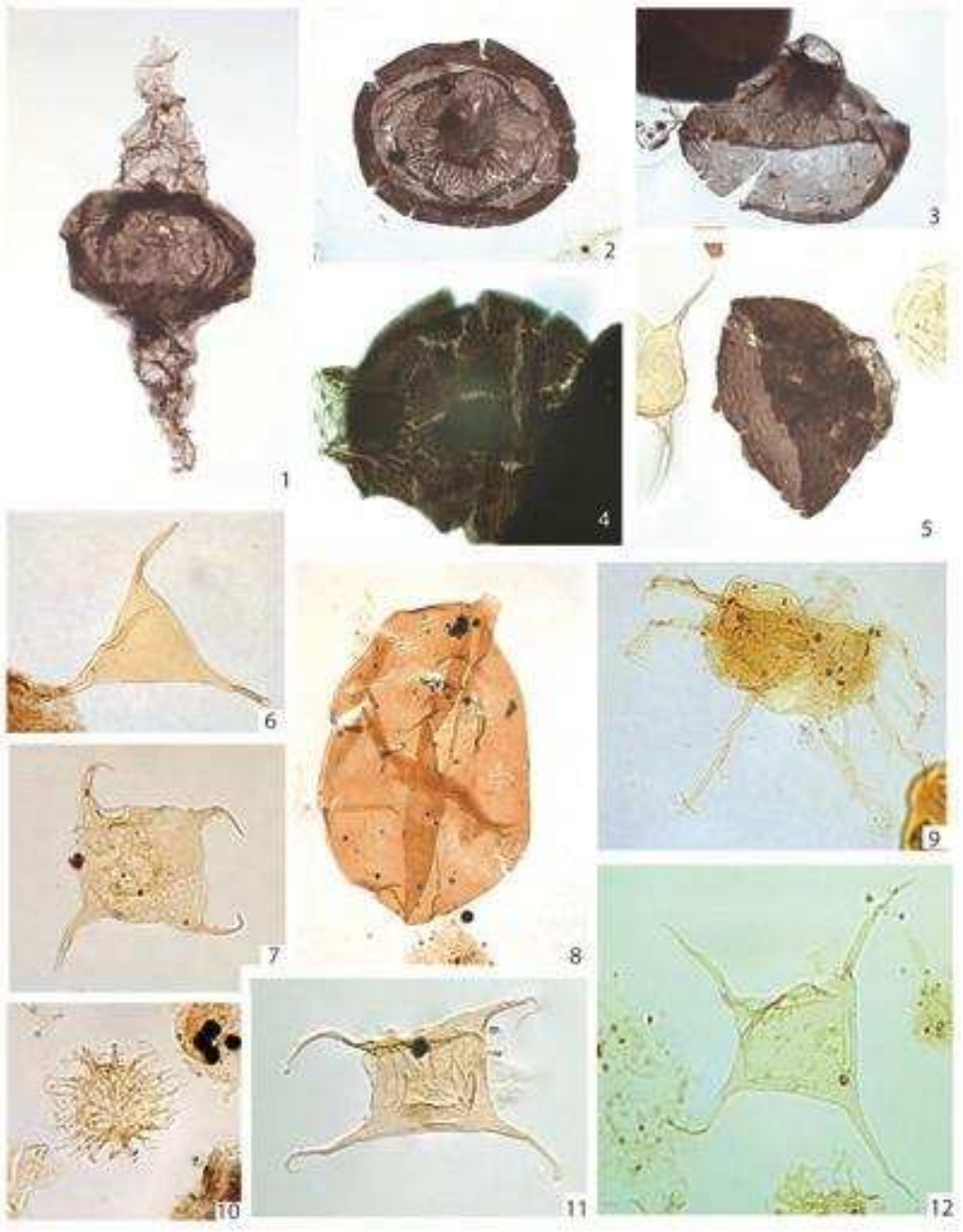

Plate 5

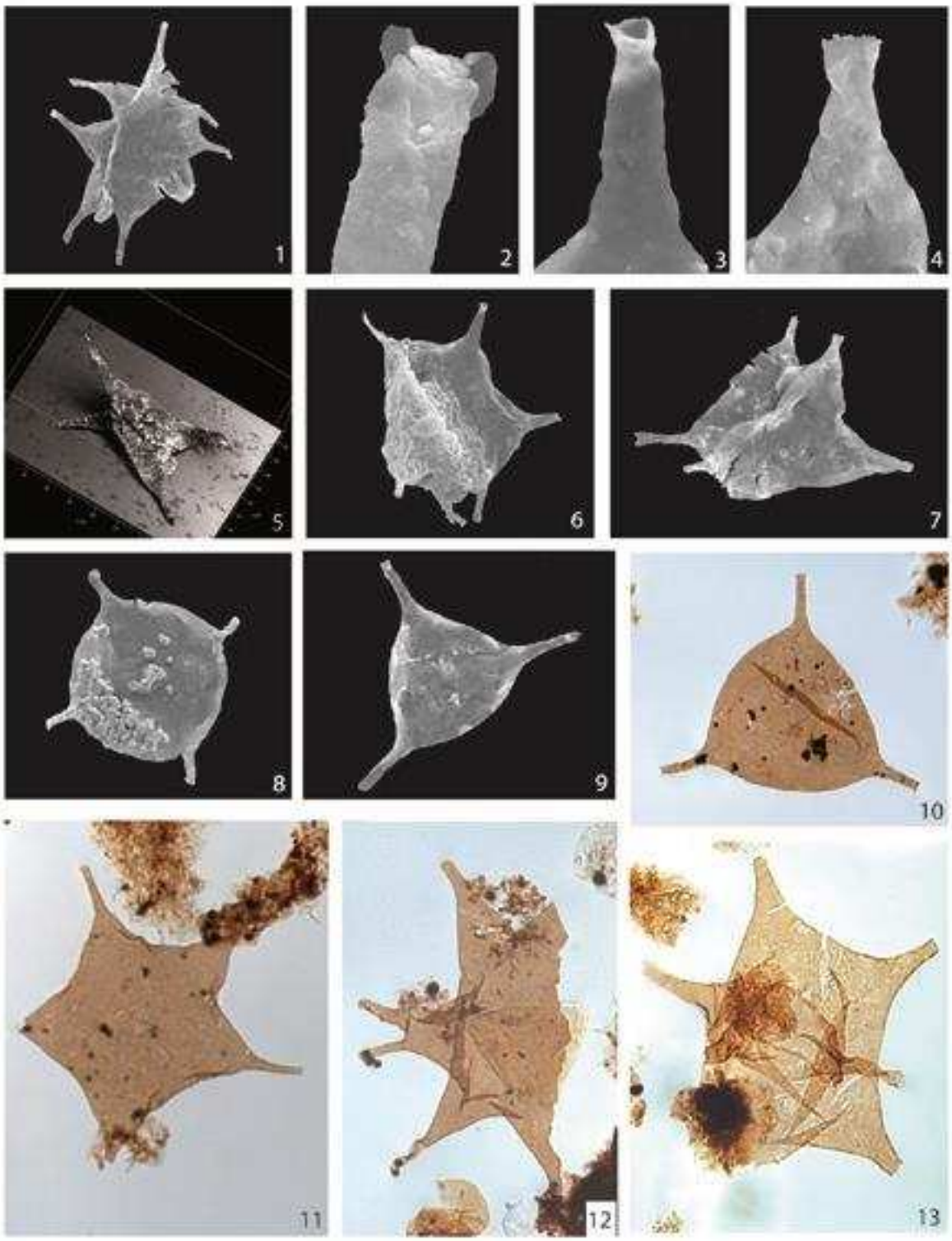

Plate 6

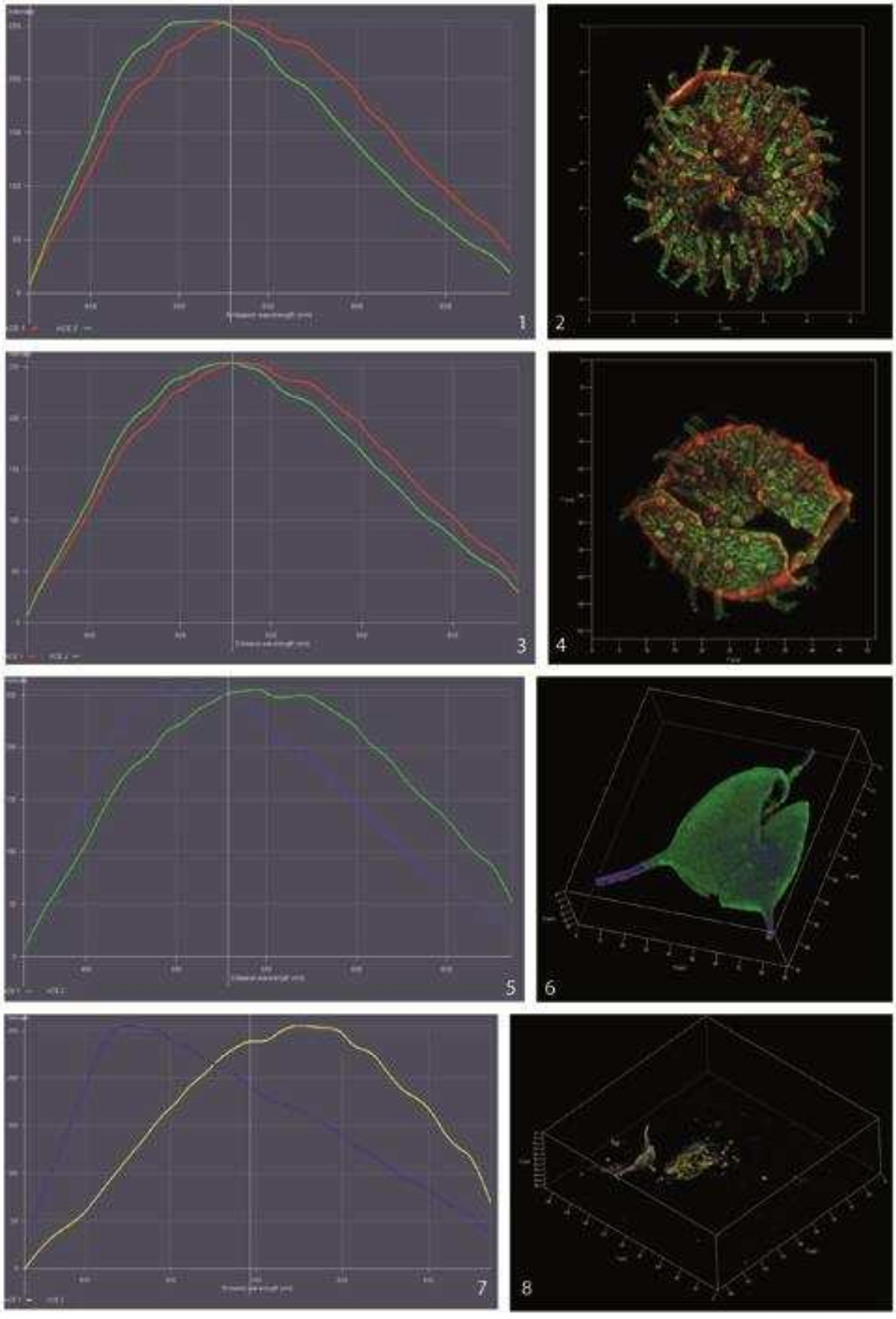

Plate 7

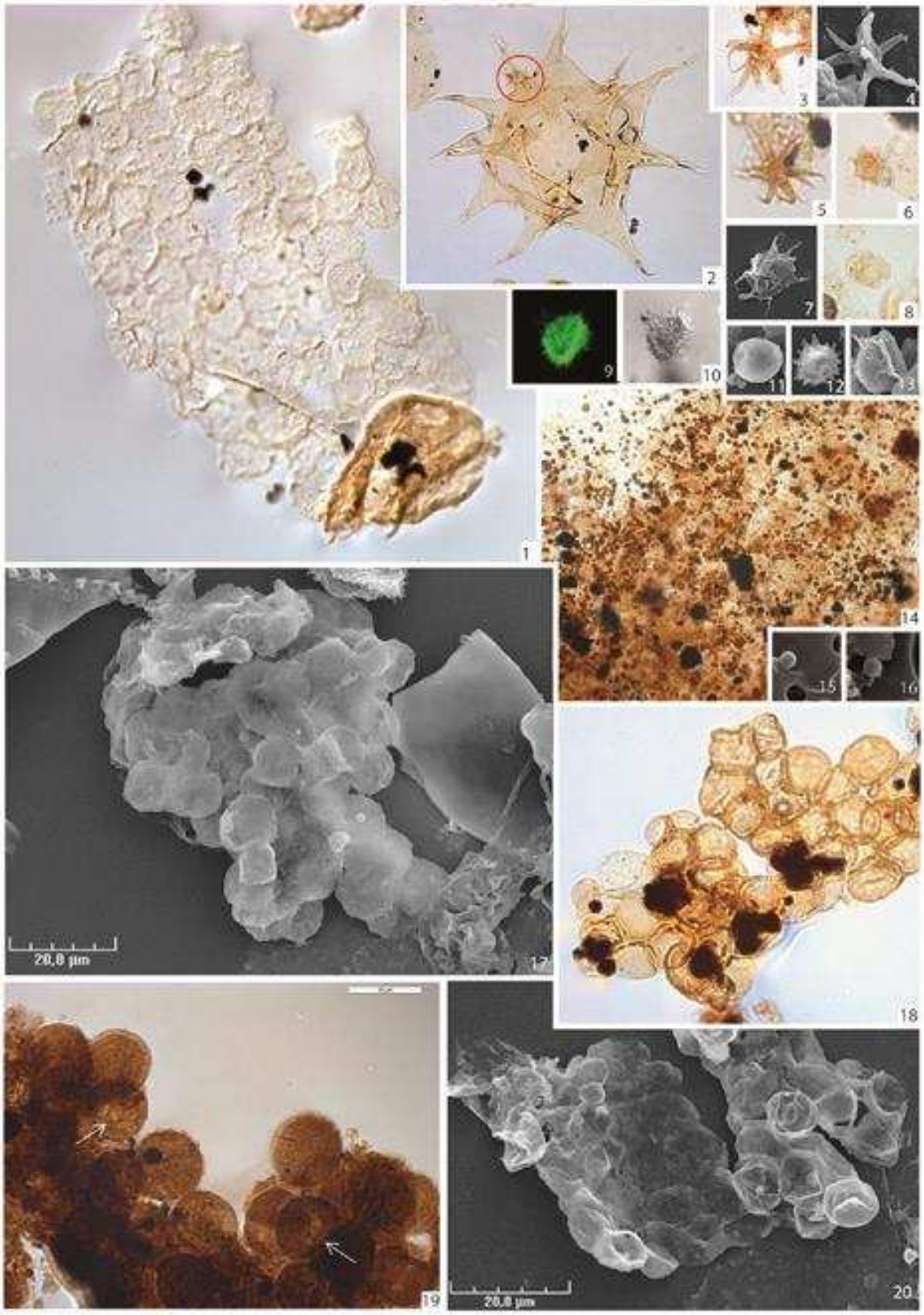

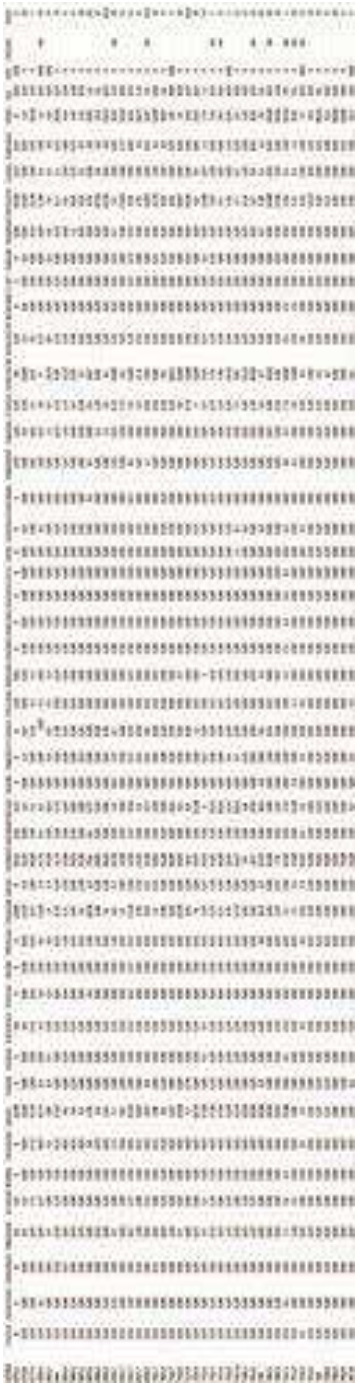

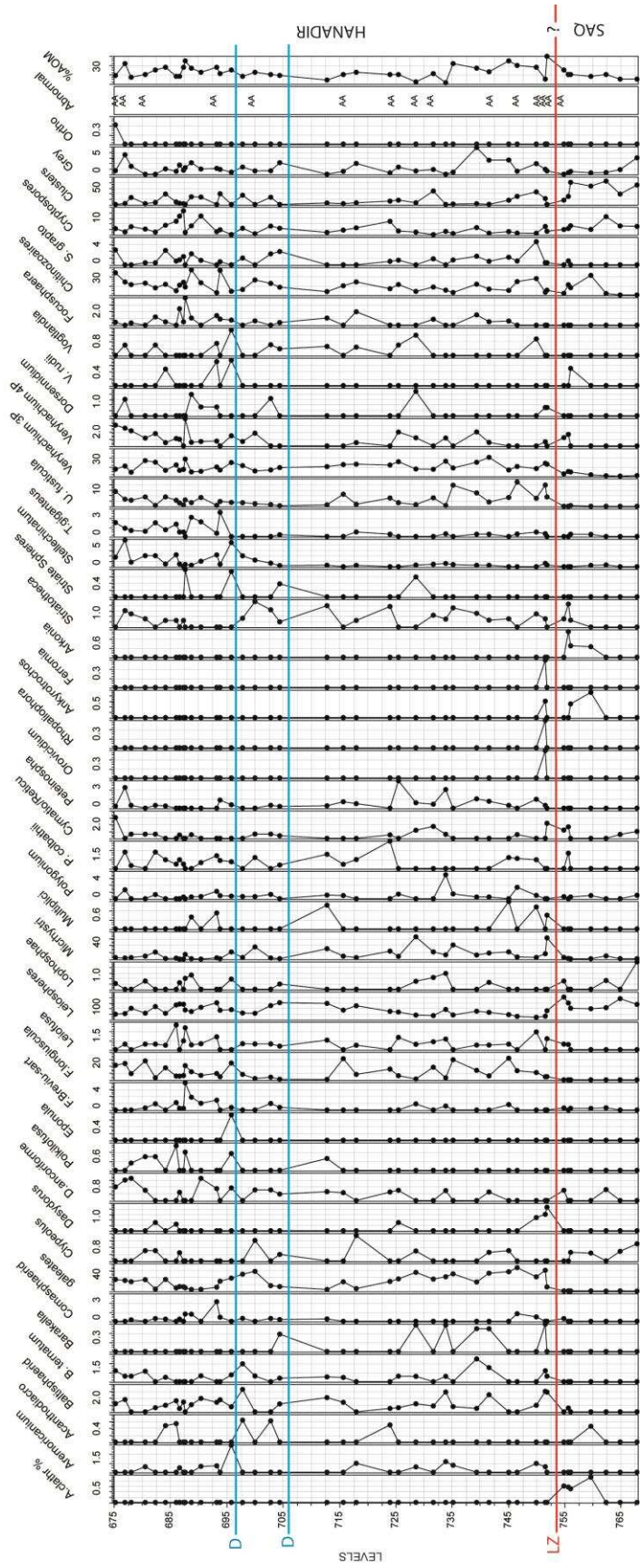
HANADIR
SAQ ?
LEVELS
D
D
LZ
%AOM
Abnormal
Chlo
Grey
Clusters
Cryptospores
S. grapio
Chlorococcales
Focusphaera
Vogtiniella
V. nudi
Dorsennidium 4p
Verynaechium 3p
U. hastucia
T.gigantieus
Selenochinatum
Striate Spheres
Strabotnea
Arconia
Ferromia
Amytrotrochos
Rhopaliophora
Oroveidium
Peleinosphs
Cmalo/Reticu
P. cobaltii
Polygonum
Multiplici
Micrysti
Lophosphaer
Leiosphaeres
Leiotasa
F.longiuscula
F.Bavlu-sart
Eponula
Pollolofusa
D.ancorifomm
Desydoms
Cryptoelus
galeates
Comasphaerid
Barakella
B. lemnatum
Balisphaerid
Azamthodacro
Aremorcanum
A.clathr %

LEVELS	galeates	GALEATE	F.longiuscu	F.LONGIL	Leiosphere	LEIOSPHI	Micrhystri	MICRHYS	Veryhachiu	VERYHAC	Cryptospor	CRYPTOS
675.1	16,95		10,65		19,13		2,17		7,6		2,17	
676.8	15,53		11,97		21,35		1,6		11,00		0,97	
677.9	13,76		4,52		40,84		2,2		4,21		2,91	
680.4	16,71		13,82		22,76		4,3		17		2,00	
682.2	3,00		1,5		47,00		10,2		15,25		0,9	
684	17,07		8,78		22,19		0,73		6,34		3,41	
685.9	4,6		2,71		52,98		1,35		12,22		4,89	
686.5	6,6		2,64		56,25		0,00		6,25		6,73	
687.2	6,3		3,1		55,36		0,00		7,3		8,7	
687.5	4,78		10,35		34,6		6,77		18,7		0,8	
688.6	2,4		5,88		28,87		0,52		4,54		3,2	
690.3	2,54		3,2		44,26		0,00		5,2		6,8	
693.1	5,7		4,6		61,00		1,8		10,00		1,05	
693.7	14,5		2,2		33,48		0,44		6,6		1,76	
695.7	18,95		12,26		35,68		10,4		14,86		0,00	
697.7	24,67		3,94		23,35		2,3		11,5		2,3	
699.9	28,9		0,93		22,36		17,7		5,59		0,31	
702.7	7,96		1,9		50,63		1,59		6,68		3,1	
704.3	6,6		0,38		61,28		0,58		9,3		2,3	
712.7	2,34		0,26		58,59		15,1		10,41		0,78	
715.6	13,58		15,45		33,95		4,2		12,64		1,63	
717.9	3,7		3,95		50,1		2,2		13,08		2,46	
723.9	14.10		7,8		29.47		11,58		12,09		4,85	
725.4	17,84		3,00		26,93		4		15,8		1,3	
728.5	27,46		0,59		15,82		32,52		7,76		0,89	
731.6	17,54		9,21		14,00		10,52		7,45		0,00	
733.8	21,00		1,45		36,44		6,12		16,32		1,16	
735.11	25,19		14,72		16,27		20,54		8,91		0,38	
739.3	13,33		6,92		30		5,9		15,12		2,56	
741.5	26,22		2,82		25,7		8,74		20,56		0,51	
745	28,36		15,8		17,54		10,5		6,7		1,1	
746.5	34,34		6,64		11,08		3,04		10,52		0,55	
749.9	20,87		5,33		7,76		2,42		8,25		0,48	
751.5	30,44		2,2		11,94		7,76		14,02		2,98	
751.8	6,08		2,3		31,88		31,00		13,04		1,2	
754.8	0,3		0,00		81,85		2,4		2,4		1,84	
755.6	0,28		0,00		60,00		0,84		5,00		2,24	
756	0,25		0,00		40,85		0,25		4,5		3,25	
759.6	0,23		0,00		39,00		0,46		1,4		1,88	
762.3	0,00		0,00		42,95		4,59		0,32		6,55	
764.8	0,28		0,00		76,00		0,56		0,00		3,17	
767.8	0,00		0,00		55,00		0,5		0,5		3,00	

No representation
Very low %
Low %
Moderate %
High %
Very high %

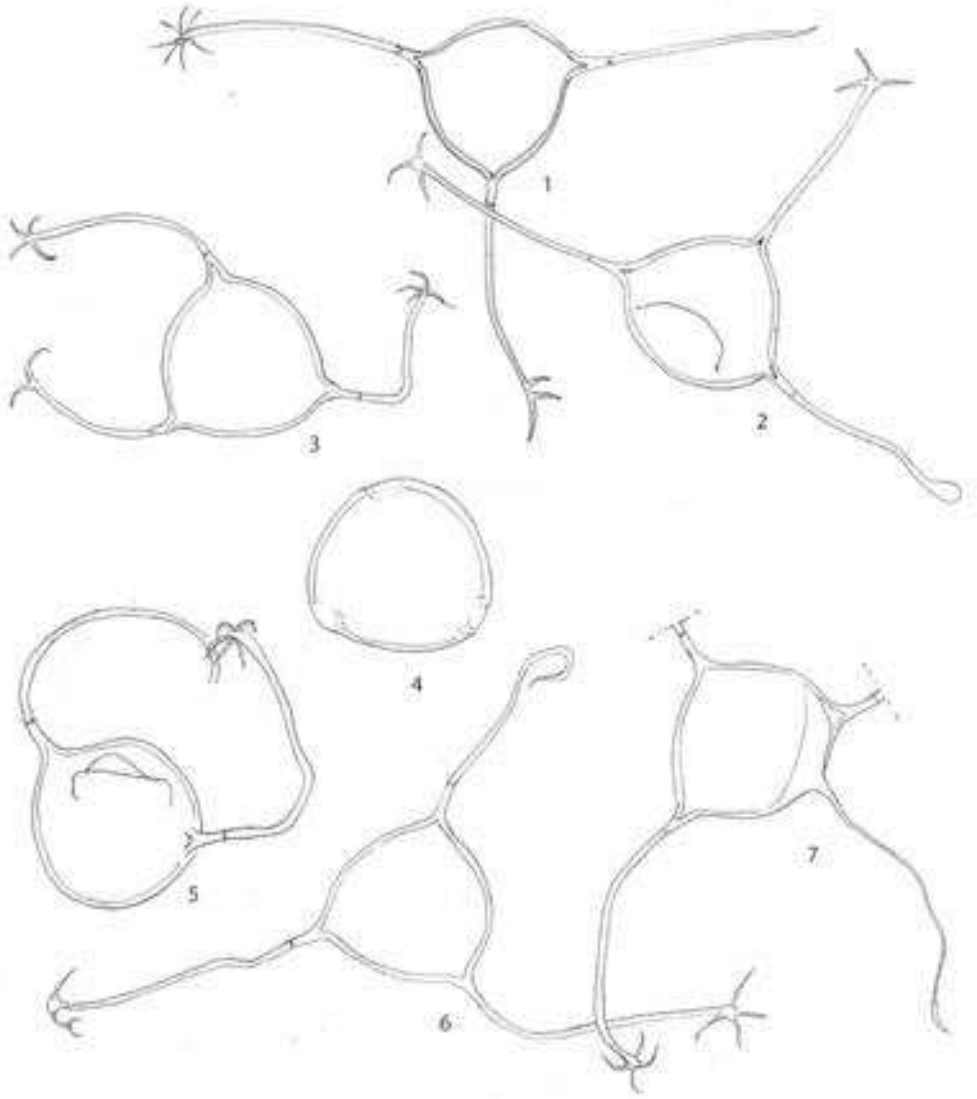
1
2
3
4
5
6
7

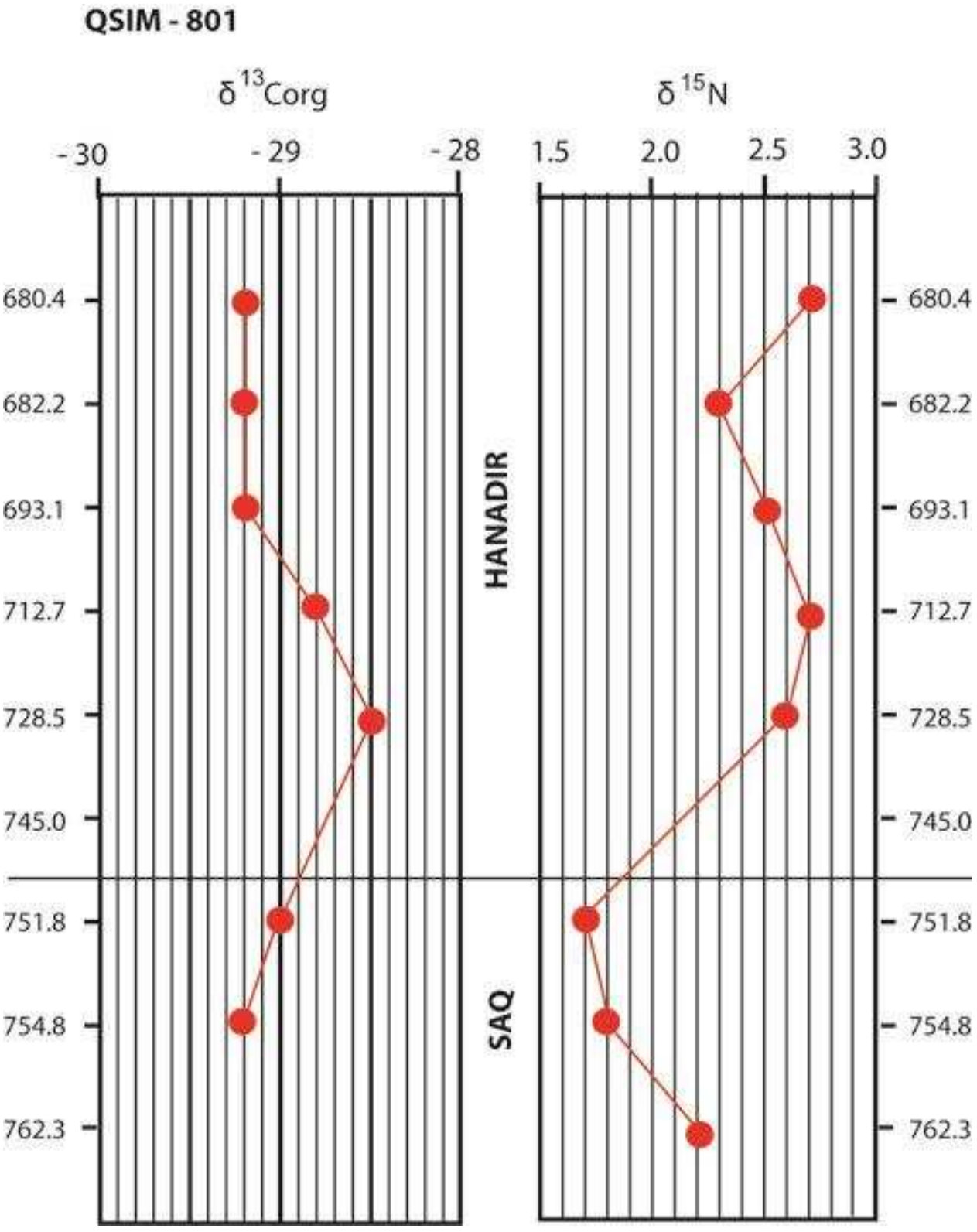
QSIM - 801
δ 13Corg
δ 15N
- 30
- 29
- 28
1.5
2.0
2.5
3.0
680.4
682.2
693.1
712.7
728.5
745.0
751.8
754.8
762.3
HANADIR
SAQ